AD_____

Award Number: DAMD17-02-1-0342

TITLE: Ron in Breast Development and Cancer

PRINCIPAL INVESTIGATOR: Susan E. Waltz, Ph.D.

CONTRACTING ORGANIZATION: University of Cincinnati
Cincinnati, OH 45221-0222

REPORT DATE: October 2006

TYPE OF REPORT: Annual Summary

PREPARED FOR: U.S. Army Medical Research and Materiel Command
Fort Detrick, Maryland 21702-5012

REPORT DOCUMENTATION PAGE

Form Approved
OMB No. 0704-0188

1. REPORT DATE	2. REPORT TYPE	3. DATES COVERED
01-10-2006	Annual Summary	1 Oct 2005 – 30 Sep 2006

4. TITLE AND SUBTITLE

Ron in Breast Development and Cancer

5a. CONTRACT NUMBER

5b. GRANT NUMBER
DAMD17-02-1-0342

5c. PROGRAM ELEMENT NUMBER

6. AUTHOR(S)

Susan E. Waltz, Ph.D.

5d. PROJECT NUMBER

5e. TASK NUMBER

5f. WORK UNIT NUMBER

7. PERFORMING ORGANIZATION NAME(S) AND ADDRESS(ES)

University of Cincinnati
Cincinnati, OH 45221-0222

8. PERFORMING ORGANIZATION REPORT NUMBER

9. SPONSORING / MONITORING AGENCY NAME(S) AND ADDRESS(ES)
U.S. Army Medical Research and Materiel Command
Fort Detrick, Maryland 21702-5012

10. SPONSOR/MONITOR'S ACRONYM(S)

11. SPONSOR/MONITOR'S REPORT NUMBER(S)

12. DISTRIBUTION / AVAILABILITY STATEMENT
Approved for Public Release; Distribution Unlimited

13. SUPPLEMENTARY NOTES
Original contains colored plates: ALL DTIC reproductions will be in black and white.

14. ABSTRACT

Not applicable

The long-term objective of this project is to define the in vivo role of the receptor tyrosine kinase Ron in mammary gland biology. Virtually nothing is known regarding the function of Ron in the breast. However, two recent studies have shown that Ron is over-expressed and highly phosphorylated in a significant fraction of human and feline breast cancers. To define the in vivo significance of Ron, mice were generated with a targeted ablation of the tyrosine kinase domain of this receptor (TK-/- mice). To determine the impact of Ron in a murine model of breast cancer, the TK-/- mice were crossed to mice expressing the polyoma virus middle T antigen (pMT) under control of the mouse mammary tumor virus promoter. Both TK-/- and control mice expressing pMT develop mammary tumors and lung metastasis. However, a significant decrease in mammary tumor initiation and growth was found in the TK-/- mice compared to controls. This decrease was associated with a significant decrease in microvessel density, decreased cellular proliferation and increased apoptosis. Biochemical analyses showed that the pMT expressing TK-/- tumors had defects in MAPK and AKT activation. Our studies are the first to demonstrate the impact of Ron signaling on tumorigenesis.

15. SUBJECT TERMS
growth factors, receptor tyrosine kinases, cancer

16. SECURITY CLASSIFICATION OF:				18. NUMBER OF PAGES	19a. NAME OF RESPONSIBLE PERSON
					USAMRMC
a. REPORT	b. ABSTRACT	c. THIS PAGE			19b. TELEPHONE NUMBER *(include area code)*
U	U	U	UU	49	

Standard Form 298 (Rev. 8-98)
Prescribed by ANSI Std. Z39.18

Table of Contents

INTRODUCTION

The purpose of my DOD funded proposal is to determine the contribution of Ron signaling in normal mammary gland growth and development (Aim 1). This is being accomplished by contrasting breast development in wild-type mice compared to mice with a block in Ron signaling. Secondly, the impact of Ron signaling in the pathogenesis of mammary gland tumors is being evaluated (Aim 2). This will be accomplished by monitoring tumor kinetics and downstream signaling cascades in a murine model of human breast cancer. During the past funding cycle, studies were focused primarily on Aim 2.

BODY

The work presented in this body is a summary of the recent findings my laboratory has generated based upon studies previously reported.

Activated growth factor receptor tyrosine kinases play pivotal roles in a variety of human cancers, including breast cancer. Ron, a member of the Met receptor tyrosine kinase protooncogene family, is overexpressed or constitutively active in 50% of human breast cancers(1). To define the significance of Ron overexpression and activation in vivo, we generated transgenic mice that overexpress a wild type or constitutively active Ron receptor in the mammary epithelium. In these animals, Ron expression is significantly elevated in mammary glands and leads to a hyperplastic phenotype by 12 weeks of age. Ron overexpression is sufficient to induce mammary transformation in all transgenic animals and is associated with a high degree of metastasis, with metastatic foci detected in liver and lungs of over 86% of all transgenic animals. Furthermore, we show that Ron overexpression leads to receptor phosphorylation and is associated with elevated levels of tyrosine phosphorylated β-catenin and the upregulation of genes, including cyclin D1 and c-myc, which are associated with poor prognosis in patients with human breast cancers. These studies suggest that Ron overexpression may be a causative factor in breast tumorigenesis and provides a model to dissect the mechanism by which the Ron induces transformation and metastasis. These results are presented in the two manuscripts included in the appendix.

Summary

Activated growth factor receptor tyrosine kinases have been shown to play pivitotal roles in a variety of human cancers. Our recent studies provide a direct demonstration that Ron receptor overexpression is sufficient to induce mammary transformation and is associated with a high degree of metastasis in a murine model of human breast cancer. These results are in agreement with human cancer studies documenting an upregulation of this receptor in breast tumors as well as are consistent with the correlation between Ron overexpression and an aggressive phenotype observed in node-negative breast tumors (2). These experiments, therefore, provide a new target for therapeutic intervention of human breast cancer. Moreover, the published manuscript included in the appendix by O'toole et al, suggests that utilizing antibodies to target Ron overexpression in human cancers may provide an effective theraputic tool.

KEY RESEARCH ACCOMPLISHMENTS

- The Ron receptor is overexpressed in a large number of tumor types and cancer cell lines.
- Ron overexpression is sufficient to induce Ron receptor phosphorylation and augmented kinase activity leading to mammary transformation.
- Mammary tumors overexpressing Ron are highly metastatic with metastases observed in the liver and lungs of the majority of animals.
- Mammary tumors derived from Ron overexpression are associated with b-catenin and MAPK activation, and increases in cyclin D1, and c-myc expression.

REPORTABLE OUTCOMES

Reportable outcomes resulting from the Career Development Award supported by the US Army Medical Research and Material Command are as follows:

Presentations at National Meetings:

Susan E. Waltz, Glendon M. Zinser, Mike A. Leonis, Kenya Toney, Peterson Pathrose, Megan Thobe, Sarah A. Kader, Belinda E. Peace, Shirelyn R. Beauman, Margaret H. Collins. Mammary-Specific Ron Receptor Overexpression Induces Highly Metastatic Mammary Tumors Associated With b-catenin Activation. 25th Congress of the International Association for Breast Cancer Research. Montreal, Canada, September 15-18,2006.

External Seminar Presentations:

"The Ron Receptor Tyrosine Kinase in Mammary Biology." Invited Speaker, McGill University, October 11-12, 2006.

"In vivo significance of Ron Receptor Signaling in Tumorigenesis and Metastasis." Invited Speaker, Genentech Inc., South San Francisco, CA, May 16, 2006.

"Ron Receptor Signaling in Mammary Tumorigenesis and Metastasis." Invited Speaker, ImClone Systems Incorporated, New York, NY March 29, 2006.

"Ron Receptor Signaling in Tumorigenesis and Metastasis." Invited Speaker, Eli Lilly and Company, Indianapolis, IN, February 21, 2006.

Publications:

O'Toole JM, Rabenau KE, Burns K, Lu D, Mangalampalli V, Balderes P, Covino N, Bassi R, Prewett M, Gottfredsen KJ, Thobe MN, Cheng Y, Li Y, Hicklin DJ, Zhu Z, Waltz SE, Hayman MJ, Ludwig DL, Pereira DS. Therapeutic implications of a human neutralizing antibody to the macrophage-stimulating protein receptor tyrosine kinase (RON), a c-MET family member. Cancer Res. 2006 Sep 15;66(18):9162-70.

Zinser, G.M.; Leonis, M.A.; Toney, K.; Pathrose, P.; Thobe, M.; Kader, S.A.; Peace, B.E.; Beauman, S.R.; Collins, M.H. and Waltz, S.E. Mammary Specific Ron Receptor Overexpression Induces Highly Metastatic Mammary Tumors Associated with β-catenin Activation. Accepted Pending Approval of Revision, Cancer Research.

Funding:

Source of Support: National Institutes of Health, R01
Assignment Number: CA100002
Title of Project: The Ron receptor in mammary gland biology
Principal Investigator: Susan E. Waltz
Award Period: 6/1/04-5/31/09
Total Direct Cost: $922,500
Percent Effort: 40%
Peer Reviewed, National, Scored 4.8 percentile

CONCLUSIONS

Although progress has been made in the detection and treatment of primary breast cancer, there still remains much to be discovered regarding mammary cell transformation and metastasis to secondary sites. Ron is a member of the MET protooncogene family, a distinct family of receptor tyrosine kinases. Receptor tyrosine kinases participate in normal mammary gland development and give rise to mammary tumorigenesis upon gene dysregulation. In this report, we utilized transgenic mice overexpressing the Ron receptor tyrosine kinase selectively in the mammary epithelium to mimic what is seen in 50% of human primary breast cancer cases. Utilizing this approach, we demonstrate that Ron overexpression is sufficient to induce the initiation and progression of mammary tumorigenesis *in vivo*. Moreover, the Ron-expressing mammary tumors are highly metastatic with metastases observed in the lung and liver of the majority of animals. These studies provide direct evidence that Ron overexpression plays a critical role in both the initiation and metastatic program of mammary tumorigenesis. Furthermore, we show that Ron overexpression within the mammary gland induces an association with β-catenin that upregulates various target genes involved in cell progression and

survival. Finally, we have supporting data published in collaboration with Imclone indicating that Ron overexpression is observed in a large fraction of human tumors and that a new humanized monoclonal antibody developed by Imclone show promise in animals models with respect to neutralizing Ron's ability to drive tumor growth.

REFERENCES

1 Maggiora, P., Marchio, S., Stella, M.C., Giai, M., Belfiore, A., De Bortoli, M., Di Renzo, M.F., Costantino, A., Sismondi, P., and Comoglio, P.M. 1998. Overexpression of the RON gene in human breast carcinoma. *Oncogene* 16:2927-2933.

2. Camp ER, Liu W, Fan F, Yang A, Somcio R, Ellis LM. RON, a tyrosine kinase receptor involved in tumor progression and metastasis. Ann Surg Oncol. 2005 Apr;12(4):273-81. Epub 2005 Mar 15.

APPENDICIES

Included in the appendix is the paper recently published in Cancer Research by O'toole et al. In addition, a second manuscript is appended that was recently revised and resubmitted to Cancer Research. Included are the comments recommending acceptance of this manuscript pending revision. These manuscripts summarize our current accomplishments in this progress report.

Therapeutic Implications of a Human Neutralizing Antibody to the Macrophage-Stimulating Protein Receptor Tyrosine Kinase (RON), a c-MET Family Member

Jennifer M. O'Toole,[1] Karen E. Rabenau,[1] Kerri Burns,[1] Dan Lu,[2] Venkat Mangalampalli,[3] Paul Balderes,[4] Nicole Covino,[4] Rajiv Bassi,[5] Marie Prewett,[5] Kimberly J. Gottfredsen,[6] Megan N. Thobe,[7] Yuan Cheng,[1] Yiwen Li,[5] Daniel J. Hicklin,[5] Zhenping Zhu,[2] Susan E. Waltz,[7] Michael J. Hayman,[6] Dale L. Ludwig,[3] and Daniel S. Pereira[1]

Departments of [1]Tumor Biology, [2]Antibody Engineering, [3]Cell Engineering and Expression, [4]Protein Sciences, and [5]Experimental Therapeutics, ImClone Systems, Inc.; [6]Department of Molecular Genetics and Microbiology, SUNY at Stonybrook, New York, New York; and [7]Department of Surgery, University of Cincinnati College of Medicine, Cincinnati, Ohio

Abstract

RON is a member of the c-MET receptor tyrosine kinase family. Like c-MET, RON is expressed by a variety of epithelial-derived tumors and cancer cell lines and it is thought to play a functional role in tumorigenesis. To date, antagonists of RON activity have not been tested *in vivo* to validate RON as a potential cancer target. In this report, we used an antibody phage display library to generate IMC-41A10, a human immunoglobulin G1 (IgG1) antibody that binds with high affinity (ED_{50} = 0.15 nmol/L) to RON and effectively blocks interaction with its ligand, macrophage-stimulating protein (MSP; IC_{50} = 2 nmol/L). We found IMC-41A10 to be a potent inhibitor of receptor and downstream signaling, cell migration, and tumorigenesis. It antagonized MSP-induced phosphorylation of RON, mitogen-activated protein kinase (MAPK), and AKT in several cancer cell lines. In HT-29 colon, NCI-H292 lung, and BXPC-3 pancreatic cancer xenograft tumor models, IMC-41A10 inhibited tumor growth by 50% to 60% as a single agent, and in BXPC-3 xenografts, it led to tumor regressions when combined with Erbitux. Western blot analyses of HT-29 and NCI-H292 xenograft tumors treated with IMC-41A10 revealed a decrease in MAPK phosphorylation compared with control IgG–treated tumors, suggesting that inhibition of MAPK activity may be required for the antitumor activity of IMC-41A10. To our knowledge, this is the first demonstration that a RON antagonist and specifically an inhibitory antibody of RON negatively affects tumorigenesis. Another major contribution of this report is an extensive analysis of RON expression in ~100 cancer cell lines and ~300 patient tumor samples representing 10 major cancer types. Taken together, our results highlight the potential therapeutic usefulness of RON activity inhibition in human cancers. (Cancer Res 2006; 66(18): 9162-70)

Introduction

The macrophage-stimulating protein receptor (RON) belongs to the c-MET family of receptor tyrosine kinases (1–3). RON ligand, macrophage-stimulating protein (MSP), was originally found to modulate the function of certain macrophage by a variety of means. For example, addition of MSP not only induced shape changes, chemotaxis, macropinocytosis, and phagocytosis (4) but also inhibited lipopolysaccharide (LPS)-induced production of inflammatory mediators such as inducible nitric oxide (5), nitric oxide (6), prostaglandins, and cyclooxygenase-2 (7). Consistent with this notion that RON negatively regulates inflammation is the observation that activated macrophages from adult RON knockout mice produced increased levels of nitric oxide both *in vitro* and *in vivo*, thus rendering them more susceptible to LPS-induced endotoxic shock (8–10). Besides macrophage, RON has also been found expressed in several normal epithelial cells such as keratinocytes (11) where MSP was shown to phosphorylate RON and activate a number of signaling pathways that elicited cell adhesion/motility and antiapoptotic and proliferative responses (12).

As is the case with its better-known family member, c-MET, several lines of evidence suggest a role for RON in cancer. First, it is highly expressed in several epithelial tumors and cell lines of the colon (13), lung (14), breast (15, 16), stomach (17), ovary (18), pancreas (3), bladder (19), liver (20), and kidney (21, 22). RON is also found coexpressed in tumors with other growth factor receptors such as c-MET and epidermal growth factor receptor (EGFR; refs. 16, 19, 23, 24). Second, MSP and RON have been shown to influence the migration and invasion of cancer cells (2, 3, 25). Third, the oncogenic potential of RON has been shown on overexpression in cultured cell lines (26–28) and in transgenic mice (29, 30) where overexpression of RON led to a profound increase in proliferation and tumorigenesis, respectively. Down-regulation of RON expression in RON-expressing cancer cell lines resulted in a reduction in proliferation (31). Similar oncogenic potential has also been observed for splice variants of RON identified in tumors and cell lines that generate receptors completely lacking the extracellular domain or that harbor deletions within this domain (26, 27, 32–35). Fourth, RON synergizes with known oncogenes. For example, the skin and breast tumorigenicity of transgenic mice overexpressing the polyoma middle T (36) and RAS (37) oncogenes, respectively, is repressed when these mice are crossed to RON knockout mice.

Whereas several antagonists of c-MET have shown antitumor activity and thus validated c-MET as a cancer target, to date, antagonists of RON activity have not shown antitumor activity to validate RON as a potential cancer target. Consequently, through the screening of a human Fab phage display library, we developed IMC-41A10, a human IgG1 monoclonal antibody that binds with

Note: Supplementary data for this article are available at Cancer Research Online (http://cancerres.aacrjournals.org/).

J.M. O'Toole and K.E. Rabenau contributed equally to this work.

Requests for reprints: Daniel S. Pereira, Department of Tumor Biology, ImClone Systems, Inc., 180 Varick Street, New York, NY 10014. Phone: 646-638-5008; Fax: 212-645-2054; E-mail: daniel.pereira@imclone.com.

doi:10.1158/0008-5472.CAN-06-0283

high affinity to human RON and blocks MSP binding. In RON-expressing cancer cell lines, we show IMC-41A10 to be a potent inhibitor of receptor signaling, cell migration, and tumorigenesis. To our knowledge, this is the first demonstration of a RON antagonist, and specifically an inhibitory antibody of RON, that negatively affects tumorigenesis. Another major contribution of this report is an extensive analysis of RON expression in ~100 cancer cell lines and ~300 patient tumor samples representing 10 and 6 major cancer types, respectively. Taken together, our results underscore the potential therapeutic usefulness of RON activity inhibition in human neoplasia.

Materials and Methods

Immunohistochemistry. The polyclonal RON (C-20) antibody from Santa Cruz Biotechnology (Santa Cruz, CA), which has previously been used to detect RON expression by immunohistochemistry (17), was used here to detect RON expression in breast (51 samples, IMH-364), lung (59 samples, IMH-305), prostate (40 samples, IMH-303), stomach (59 samples, IMH-316), and colon (59 samples, IMH-306) tumor tissue arrays purchased from Imgenex (Sorrento Valley, CA). Pancreatic tumor tissue arrays (54 samples, CC1401) were obtained from Cybrdi (Frederick, MD). These formalin-fixed paraffin-embedded arrays were treated and stained with 1.2 μg/mL RON (C-20) antibody or rabbit IgG as a negative control (Jackson Immuno-Research Laboratories, West Grove, PA) using the EnVision+ Rabbit Kit (DAKO, Carpinteria, CA) as described (38).

Cell culture. Cell lines used in this study were obtained from the American Type Culture Collection (Manassas, VA) and grown exactly as recommended. Media used for their propagation were purchased from Life Technologies, Inc. (Grand Island, NY).

Flow cytometry. To measure cell-surface expression of RON, cancer cell lines were grown to subconfluence, trypsinized, washed, pelleted (5 minutes, 1,400 rpm), and resuspended/filtered in 250 μL PBS + 5% fetal bovine serum (FBS). Five micrograms of RON antibody (IMC-41A10) were added to all tubes, except the control tube, and incubated for 30 minutes at 4°C. Cells were washed, pelleted (5 minutes, 1,400 rpm), and resuspended in 250 μL PBS + 5% FBS. One microgram of the secondary antibody, goat anti-human IgG-phycoerythrin (Jackson ImmunoResearch Laboratories), was added and left for 30 minutes at 4°C. Finally, cells were washed, pelleted, and resuspended in 500 μL PBS + 5% FBS for analysis on a Becton Dickinson (San Jose, CA) FACSVantage SE.

Identification of human anti-RON Fab antibodies from a phage display library. A human Fab phage display library containing 3.7×10^{10} clones (39) was used to screen for and identify human anti-RON Fab antibodies following a previously described procedure (40) using RON-Fc (Sigma-Aldrich, St. Louis, MO) as the bait. Individual phage clones recovered after the second and the third round of selections were examined for binding to immobilized RON-Fc by ELISA. Plasmids of individual binders were then used to transform a nonsuppressor *Escherichia coli* host HB2151 for the expression of soluble Fab fragments. The soluble Fab proteins were purified from the bacteria periplasmic extracts by affinity chromatography using a Protein G column, following the protocol of the manufacturer (Amersham Pharmacia Biotech, Piscataway, NJ), and tested for binding to RON-Fc by ELISA.

In MSP/RON blocking assay, Maxi-sorp 96-well microtiter plates (Nunc, Rochester, NY) were coated with MSP (1 μg/mL × 100 μL; R&D Systems, Minneapolis, MN) at room temperature for 1.5 hours. After washing the wells, they were blocked with 3% PBS/milk. Anti-RON antibodies (Fab or full IgG) were preincubated with RON-Fc (25 ng/well) at room temperature for 1 hour. The Fab/RON-Fc or IgG/RON-Fc mixtures were then added to the MSP-coated wells and allowed to incubate for 1.5 hours at room temperature. After several washes, a 1:1,000 dilution of the antihuman IgG, Fab-specific horseradish peroxidase (HRP)–conjugated antibody was added to the plates for 1.5 hours at room temperature to detect the anti-RON Fab or IgG that bound to RON but did not block the MSP/RON interaction. IMC-41A10 and IMC-42E12 are examples of antibodies that blocked and failed to block the MSP/RON interaction, respectively.

ELISA to detect binding of IMC-41A10 to RON. Standard ELISA plates were coated overnight at 4°C with recombinant human MSPR (R&D Systems) at 100 ng/well. The plates were washed once with 0.2% PBS/T and blocked with 3% milk (150 μL/well) for 1 hour at 37°C. Following a wash with 0.2% PBS/T, a 3 nmol/L solution of IMC-41A10 was prepared in 1 mL 3% milk and diluted 1:2 across plates. The plates were incubated for 1 hour at room temperature on a rocker and washed five times with 0.2% PBS/T. The secondary antibody (goat anti-human Fc, HRP-conjugated) was added at 1:5,000 dilution and allowed to incubate for 1 hour at room temperature. Washing was done as above. One hundred microliters of substrate were added per well until a yellow color developed. The reaction was stopped with 50 μL of 1 N H_2SO_4 and the absorbance at 450 nm determined with a standard plate reader.

To determine whether IMC-41A10 could cross-react with c-MET [hepatocyte growth factor receptor (HGFR)], an ELISA was done exactly as described above with the exception that a recombinant human HGFR (c-MET)/Fc chimeric protein (R&D Systems) was used to coat the plates and a mouse anti-human HGFR antibody (R&D Systems) was used as a positive control. A goat anti-mouse HRP antibody was used as the secondary antibody for the positive control.

ELISA to detect IMC-41A10 blocking of MSP binding to RON. ELISA plates were coated with 100 ng/well carrier-free MSP (R&D Systems) overnight at 4°C on a rocker. The plate was washed once with 0.2% PBS/T and blocked for 2 hours at 37°C with 150 μL/well 3% milk. A 15 μg/mL dilution of IMC-41A10 was prepared and serially diluted across another ELISA plate. To the IMC-41A10, we added 100 ng/well recombinant human MSPR (R&D Systems). The IMC-41A10/rh-MSPR complex was allowed to form for 2 hours at room temperature on a rocker. Next, the MSP-coated ELISA plate was washed once with 0.2% PBS/T and 100 μL of the IMC-41A10/rh-MSPR complex were added per well. After a 1.5-hour incubation at room temperature, the plate was washed five times with 0.2% PBS/T and incubated for 1 hour at room temperature with a 1:2,000 dilution of anti–His-tag HRP antibody (Sigma), which recognizes a His tag on the recombinant human MSPR protein. The plate was washed five times with 0.2% PBS/T and 100-μL substrate was added per well until a yellow color developed. The reaction was stopped with 50 μL of 1 N H_2SO_4 and the absorbance at 450 nm determined with a standard plate reader.

Analysis of MSP-induced phosphorylation of RON, mitogen-activated protein kinase, and AKT. Cells were grown in six-well plates or 10-cm dishes to ~70% confluency and serum starved for 18 hours. For cells receiving antibody, 100 nmol/L 41A10 or 42E12 was added and incubated at 37°C for 1 hour. MSP (R&D Systems) was then added to the appropriate cells at 10 nmol/L and incubated for 30 minutes at 37°C. Cells were washed twice with ice-cold PBS and lysates prepared in ice-cold cell extraction buffer (Biosource International, Carlsbad, CA) plus fresh HALT protease inhibitor cocktail (Pierce, Rockford, IL) and 15 μg of lysates were resolved by SDS-PAGE using 4% to 12% NuPAGE Novex Bis-Tris Gels with 1× MOPS running buffer. For Western blotting, proteins were transferred to a nitrocellulose membrane (Invitrogen, Carlsbad, CA) and blocked with 5% nonfat milk in TBS/0.1% Tween 20 (TBS-T) for 1 hour at room temperature on a rocker. After three 5-minute washes with TBS-T, the membrane was incubated with 1:1,000 rabbit polyclonal phospho-p44/42 MAPK (Thr^{202}/Tyr^{204}) antibody (Cell Signaling, Danvers, MA) diluted in 1% nonfat milk in TBS-T or 1:500 rabbit polyclonal anti-phospho-AKT ($P\text{-}Ser^{472/473/474}$) antibody (BD PharMingen, San Jose, CA) or 1:1,000 rabbit monoclonal phosphor-AKT (Ser^{473}) antibody (Cell Signaling). Following three 5-minute washes with TBS-T, a 1:5,000 dilution of anti-rabbit IgG, HRP-conjugated secondary antibody (Amersham) was added to the membrane for 1 hour at room temperature followed by three 5-minute TBS-T washes. Protein bands were detected with Amersham Enhanced Chemiluminescence Western Detection Kit. To determine expression levels of mitogen-activated protein kinase (MAPK), these membranes were stripped with Pierce Restore Western Blot Stripping Buffer (15 minutes at room temperature) and reprobed with a 1:1,000 dilution of p44/42 MAPK polyclonal rabbit antibody (Cell Signaling) or a 1:500 dilution of polyclonal rabbit anti-AKT1 antibody (BD PharMingen) or 1:2,000 rabbit polyclonal anti-AKT antibody (Cell Signaling).

Table 1. RON expression in patient tumor samples as determined by immunohistochemistry analysis of tumor tissue arrays

Cancer tissue	%Positive*	Mean intensity †
Breast	100% (47 of 47)	166 (20-300)
Lung	93% (50 of 54)	142 (15-300)
Prostate	92% (35 of 38)	164 (20-300)
Gastric	73% (38 of 52)	172 (20-300)
Pancreas	69% (36 of 52)	100 (30-200)
Colon	65% (36 of 55)	54 (15-225)

*The percentage of RON-expressing tumor samples on the tumor tissue array is listed. In parentheses, the numerator represents the number of RON-expressing tumor cores and the denominator equals the total number of tumor cores present on the tumor tissue array.
† Mean intensity represents tumor epithelial staining intensity in RON-positive samples. This value is obtained by multiplying a relative intensity score (0-3) by the percentage of epithelial cells present in the sample core. See Materials and Methods for experimental details.

RON-NIH3T3 cells were used to detect MSP-induced phosporylation of RON. The procedure used was exactly as described above with the exception that cells were serum starved for 2.5 hours and stimulated with or without 10 nmol/L MSP for 30 minutes at 37C. Before MSP stimulation, RON antibodies were added to cells for 1 hour at 100 nmol/L to assess blocking activity. To determine whether RON antibodies exhibited agonist activity on RON phosphorylation, antibody was added to cells in the absence of MSP stimulation. Cells were lysed and 30 μg of lysate were resolved on a 4% to 12% gel. Western blot analysis was done with anti-phosphotyrosine antibody, 4G10 (Upstate, Charlottesville, VA), as per recommendation of the manufacturer.

Cell migration assay. To determine whether IMC-41A10 could block the migration of H596 cells induced by MSP, we used cell culture inserts containing porous translucent polyethylene terephthalate track–etched membranes (8.0 μm pore size; Becton Dickinson Falcon). Before the assay, the undersides of the porous membranes in the cell culture inserts were coated with collagen by placing them into a 24-well Falcon plate filled with 700 μL of Vitrogen-100 purified collagen solution (25 μg/mL; Cohesion, Palo Alto, CA). The inserts were left for at least 1 hour at 4°C and placed in a new 24-well plate containing either 700-μL serum-free medium or 10% FBS. Next, 6×10^5 viable cells that had been serum starved for 24 hours were rinsed twice with PBS and seeded into the upper chamber of the cell culture insert in 300 μL of serum-free medium. MSP was added to the lower chamber for 24 hours at 37°C to induce cell adhesion and migration through the collagen-coated porous membrane on the underside of the cell culture insert. Before the addition of MSP, IMC-41A10 was added to other wells to determine if it could inhibit the MSP-induced migration/invasion of H596 cells. IMC-42E12, which binds to RON but does not block MSP binding, was used as a negative control. At the conclusion of the assay, migrated cells present on the underside of the collagen-coated membrane were stained with H&E and visualized by bright field microscopy at ×100 magnification.

***In vitro* "wound" healing assay.** HCA-7 cells were seeded at 2×10^6 in a 4-mL suspension in a 60-mm tissue culture dish and allowed to grow to confluence, refreshing the medium every 3 to 4 days. When 41A10 or anti–keyhole limpet hemocyanin (KLH) antibodies were used, the cells were preincubated with the antibodies for 1 hour before wound infliction. At the start of the assay, a small wound was inflicted with a plastic pipette tip. The cells were incubated for 24 hours with and without the presence of MSP plus anti-KLH or anti-RON (41A10) antibodies. The cells were imaged on a Zeiss microscope immediately after wounding (time 0) and at 16 and 24 hours.

Tumor xenograft models. To establish tumor xenograft models with which to test the antitumor activity of IMC-41A10, 5 million HT-29, NCI-H292, and BXPC-3 cells were mixed with Matrigel (Collaborative Research Biochemicals, Bedford, MA) and s.c. injected into the left flank of 56-week-old female athymic (*nu/nu*) mice (Charles River Laboratories, Wilmington, MA). Tumors were allowed to reach 150 to 300 mm^3 in size and mice were randomized into groups of 12 animals each. Mice were treated by i.p. injection every 3 days with control antibody (human IgG) or IMC-41A10 antibody at a dose of 40 mg/kg or Erbitux at a dose of 40 mg/kg. Treatment of animals was continued for the duration of the study. Tumors were measured twice each week with a caliper and tumor volumes calculated using the following formula: $(\pi/6\ (w_1 \times w_2 \times w_2))$, where w_1 represents the largest tumor diameter, and w_2 represents the smallest tumor.

Analysis of MAPK activity in HT-29 and NCI-H292 tumor xenografts. HT-29 and NCI-H292 tumor xenografts were established as described above with the exception that six mice were used for IMC-41A10 treatment and six used for control IgG treatment. Once tumors reached ~300 mm^3, mice were injected once with an antibody dose of 40 mg/kg. After 24 hours, mice were sacrificed and tumors excised. Tumor lysates were prepared and subjected to Western blot analysis. To determine whether IMC-41A10 had an effect on MAPK activity, phosphorylated and total MAPK levels were detected as described above and subjected to densitometric analysis. The densitometric values for the total MAPK bands were normalized to 20,000 and, in turn, the densitometric values of the phosphorylated MAPK bands were proportionately adjusted. The adjusted phosphorylated MAPK values for the six IMC-41A10 mice were averaged and compared with those of the six control IgG mice. Statistical significance between the two groups was determined by Student's t test.

Results

RON is expressed in several cancerous tissues and cell lines. We did an extensive analysis of RON expression in several cancer tissues by tumor tissue arrays as well as in cell lines by flow cytometry and Western blot analyses. In addition, through access to the Gene Logic Ascenta database, we were able to assess RON expression profile in a variety of cancer tissues as well as in the NCI-60 cancer cell line panel. Table 1 is a summary of RON expression in human cancer as determined by immunohistochemistry of Imgenex tumor tissue arrays. RON was expressed in 100%, 93%, 92%, 73%, 69%, and 65% of breast, lung, prostate, gastric, pancreas, and colon tumors, respectively. Table 1 also shows the mean intensity of RON expression in the tumor epithelial cells for each of these cancer types. Figure 1 is a montage of tumor tissue sections from these tumor tissue arrays that exhibit a mean epithelial cell intensity of RON expression similar to that listed in Table 1. Patient information for the tumor tissue sections shown in Fig. 1 is given in the figure legend. With respect to cancer cell lines, Table 2 lists those that are positive and negative for RON expression on the basis of flow cytometry, Western blotting, and Ascenta data (Gene Logic). Of the ~100 cell lines tested that cover 10 different cancer types, approximately half exhibited RON expression. Interestingly, none of the leukemic and renal cancer cell lines expressed RON by these analyses.

Identification and characterization of IMC-41A10 as an antibody that binds to RON and blocks its interaction with MSP. To determine whether RON plays a functional role in tumor growth, we generated a neutralizing monoclonal antibody. For this task, a human Fab antibody/phage display library was used to isolate fully human high-affinity antibodies capable of binding the RON receptor and blocking ligand binding (data not shown). To begin this process, an Fc fusion protein of the extracellular portion of the RON receptor was used to screen the Fab phage display

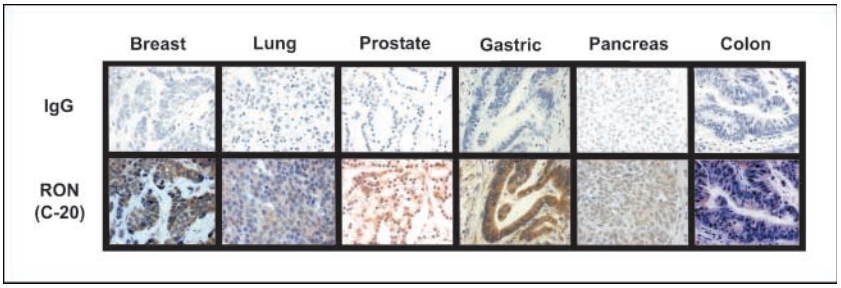

Figure 1. Montage of immunohistochemistry images from the tumor tissue array analysis of RON expression described in Table 1. The images shown in this figure were chosen to match the mean expression intensity of RON reported for each cancer type in Table 1. Patient data corresponding to the tumor images are as follows: Breast (infiltrating ductal carcinoma, stage T_{4b}), Lung (adenosquamous carcinoma, stage IIIA, $T_2N_2M_0$), Prostate (adenocarcinoma, stage III, $T_3N_0M_0$), Gastric (stage IB, $T_2N_0M_0$, well differentiated), Pancreas (ductal adenoma, stage III), and Colon (sigmoid adenocarcinoma, stage II, $T_3N_0M_0$, moderately differentiated).

library, which contains $\sim 10^7$ naïve recombinant Fab fragments. Following three rounds of selection, binding Fab fragments were identified. Four of these were subsequently found to efficiently block the interaction of MSP ligand with RON. Following the cloning of these Fabs into mammalian expression vectors harboring the fully human IgG1 backbone, one antibody, IMC-41A10, was chosen for further studies.

To quantitate the binding and blocking potential of IMC-41A10 to RON, ELISA assays were established. ELISA data revealed a receptor binding ED_{50} of 0.15 nmol/L and a receptor blocking IC_{50} of 2 nmol/L for IMC-41A10 (Fig. 2*A* and *B*). Because RON is a member of the c-MET receptor family, we wanted to determine whether IMC-41A10 could also bind c-MET. Using an ELISA-based binding assay with immobilized soluble extracellular c-MET protein, we showed that IMC-41A10 could not bind c-MET (Fig. 2*C*).

IMC-41A10 significantly inhibits MSP-dependent phosphorylation of RON and downstream signaling. Once IMC-41A10 was shown to function in solid-phase receptor binding and blocking assays, we evaluated its ability to block the activity of the RON receptor and the downstream effectors, MAPK and AKT, in cell-based assays. To assess the ability of IMC-41A10 to inhibit RON phosphorylation, we used NIH3T3 cells overexpressing the recombinant wild-type RON protein (Fig. 3*A*). When these cells were serum starved and stimulated with MSP, tyrosine phosphorylation of RON was readily detected and could be significantly inhibited ($\sim$75%) by the addition of IMC-41A10. In contrast, no inhibition of RON phosphorylation was noted with IMC-42E12 (an antibody that binds to RON but does not block MSP binding to RON). It is important to note that when 41A10 was added to the RON-NIH3T3 cells in the absence of MSP (Fig. 3*A, lane 3*), no induction of RON phosphorylation was observed, indicating that IMC-41A10 is devoid of agonist activity on the RON receptor. Because the MSP/RON pathway is known to affect MAPK and AKT activity, we were interested in evaluating the potential of IMC-41A10 to inhibit the phosphorylation and subsequent activation of MAPK (Fig. 3*B*). Using cell lines that represent a number of different cancers [i.e., HT-29 (colon), NCI-H292 (lung), HCC-1937 (breast), BXPC-3 (pancreas), DU145 (prostate), and AGS (gastric)], we determined that IMC-41A10 was able to completely inhibit MSP-induced phosphorylation of MAPK in every case and of AKT in HT-29, DU145, and AGS cells. Following MSP treatment, AKT phosphorylation did not occur in NCI-H292, BXPC-3 and HCC-1937 cells. It is also interesting to note that for many of the aforementioned cell lines, constitutive phosphorylation of MAPK and AKT was noted in the absence of exogenously added MSP.

IMC-41A10 significantly inhibits cell migration. Like HGF and c-MET, MSP and RON have been implicated in the migration and invasion of certain macrophage and epithelial cells. Previously, MSP was shown to induce migration of the H596 lung cancer cell line *in vitro* (14). We modified this assay (Fig. 4*A*) and tested the

Table 2. Flow cytometric, Western blot, and Gene Logic analyses of RON expression in cancer cell lines

Tumor type	Positive cell lines	Negative cell lines
Colon	DiFi, HCT-8, HCT-15, HCT-116 HCC-2998, Colo205, Colo-201 DLD-1, GEO, T84, HT-29, KM12 Sw480, Sw620	SNU-C1, LoVo, CaCo-2
Lung	NCI-H1650, NCI-H292, NCI-H1975, NCI-H358, NCI-H1666, NCI-H226, NCI-H441, NCI-H1650, NCI-H727, NCI-H596, NCI-H322M, EKVX, A549	NCI-H460, NCI-H23, NCI-H522 Hop-62, Hop-92
Pancreas	BXPC-3, Capan-2, HPAC, HPAFII L3#7.p1, Hs766.T, ASPC-1, CFPAC-1	MIA-PACA-2
Breast	T47D, HCC-1937, MDA-MB-468, BT20, DU4475	MDA-MB-231, MDA-MB-435, MCF-7, BT-474, SKBR3, Hs578T
Ovary	SKOV3, OVCAR3, OVCAR5, MDAH-2774, IGOV-1, OV90	OVCAR8, CaCOV3, CaCOV4
Prostate	PC-3, DU145, LnCAP	22RV.1
Stomach	NCI-N87, AGS	SNU-1, SNU-16, KKVR
Liver	HepG2	SNU-182, SNU-449, SNU-475 SNU-398, Hep3B, PLC/PRF/5
Leukemia		EOL, JM-1, HEL, Jurkat, TF-1 U937, HL-60
Kidney		A498, Caki-1, SKRC29, 786-0, ACHN, RXF-393, SN12C, TK-10, UO-31

NOTE: Of the cell lines present in the NCI-60 cancer cell line panel, expression analysis was collected from Gene Logic's Ascenta database, which contains Affymetrix expression data for the NCI-60 cancer cell line panel. These data were accessed through an institutional subscription to the Ascenta database.

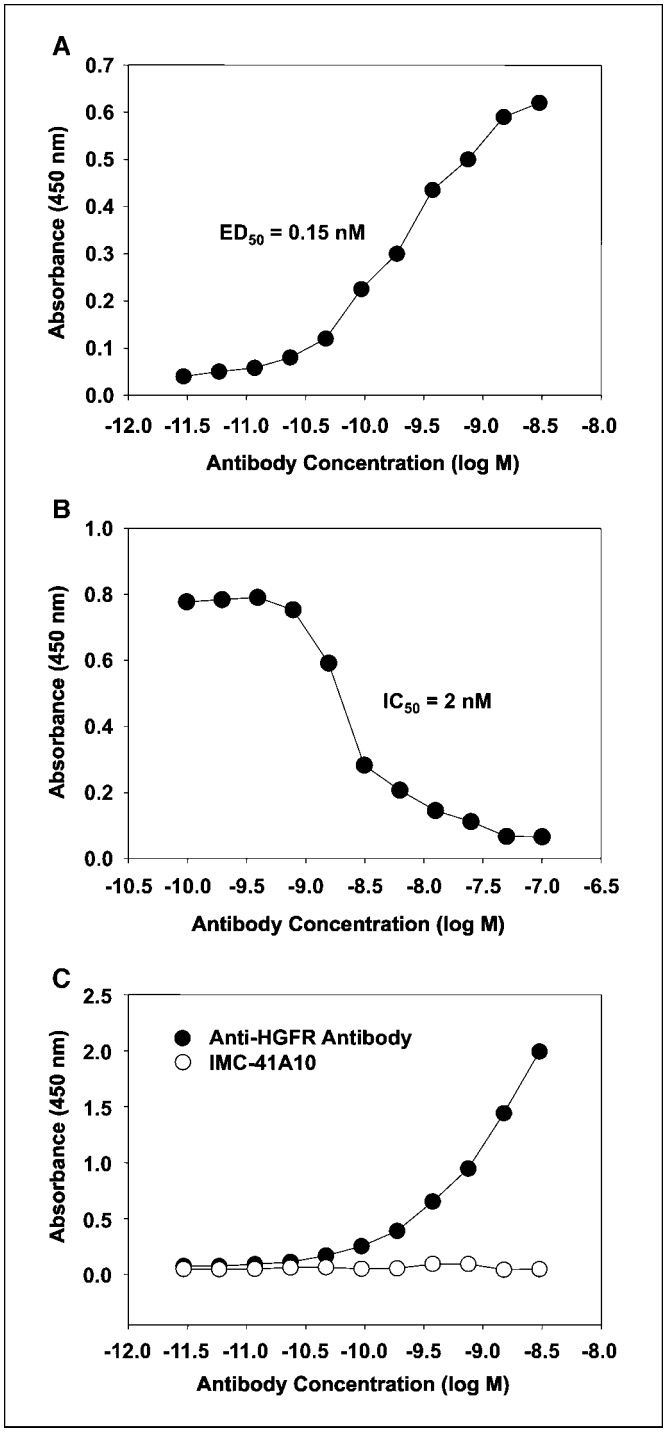

Figure 2. Solid-phase binding and blocking characteristics of IMC-41A10. *A,* ELISA to determine the ED_{50} of IMC-41A10 binding to immobilized rh RON protein. *B,* ELISA to determine the IC_{50} of IMC-41A10 needed to block the interaction of recombinant human MSP to immobilized recombinant human RON protein. *C,* ELISA to determine whether IMC-41A10 can bind to immobilized recombinant human c-MET protein. An antihuman HGFR (c-MET) antibody is used as a positive control.

ability of IMC-41A10 to inhibit MSP-induced migration of H596 cells. In comparison with IMC-42E12, IMC-41A10 showed >90% inhibition of MSP-mediated cell migration (Fig. 4*B*). These data are shown graphically in Supplementary Fig. S1. Using an *in vitro* wound healing assay, we also showed that IMC-41A10 could significantly inhibit (~75%) the ability of HCA7 colon cancer cells to migrate in response to MSP and close a "wound" created in their monolayer (Fig. 4*C*). Taken together, these data confirm that MSP-dependent tumor cell migration can be inhibited by antagonizing MSP binding to RON.

IMC-41A10 possesses antitumor activity. Because IMC-41A10 successfully abrogated RON signaling and cell migration/invasion, we were interested in determining whether it could inhibit tumorigenicity. To begin to test the antitumor activity of IMC-41A10, murine tumor xenograft models were established using HT-29 colon, NCI-H292 lung, and BXPC-3 pancreatic cancer cells. These cells were s.c. injected into nude mice and tumors allowed to establish to a size of ~250 mm^3 before being randomized into treatment groups. IMC-41A10 and a control human IgG were subsequently injected i.p. at a dose of 40 mg/kg every 3 days. In comparison with control IgG-injected mice, IMC-41A10 treatment led to a 58%, 50%, and 50% inhibition of HT-29, NCI-H292, and BXPC-3 tumor growth, respectively (Fig. 5*A-C*). It should be noted that no differences in tumor necrosis were observed in control IgG versus IMC-41A10-treated tumors (see Supplementary Fig. S2 for examples of HT-29 tumor xenografts).

To determine whether IMC-41A10 could be more efficacious in HT-29 xenografts, we initiated a subcutaneous prophylactic murine tumor xenograft model where IMC-41A10 was administered at 40 and 80 mg/kg every 3 days commencing 1 day after HT-29 cells were injected (Supplementary Fig. S3). IMC-41A10 did not exhibit increased efficacy in this model versus the established subcutaneous HT-29 tumor xenograft model in Fig. 5*A*.

IMC-41A10 inhibits phosphorylation of MAPK in HT-29 and NCI-H292 tumor xenografts. Because IMC-41A10 was shown to inhibit MAPK phosphorylation in cultured HT-29 and NCI-H292 cells (Fig. 3), we were interested in confirming whether MAPK signaling was also inhibited in xenograft tumors of IMC-41A10-treated mice. After treating established HT-29 and NCI-H292 tumors with a single 40 mg/kg dose of IMC-41A10, tumor lysates were prepared after 24 and 72 hours, respectively, to quantitate MAPK phosphorylation levels by Western blot analysis. We found that IMC-41A10 treatment of HT-29 and NCI-H292 xenografts resulted in a 35% and 28% mean decrease in phosphorylated MAPK levels compared with control IgG-treated tumors (Fig. 6). IMC-41A10-treated HT-29 tumors 2, 4, and 5 as well as NCI-H292-treated tumors 1, 2, and 4 showed phosphorylated MAPK levels below that of any of the IgG-treated tumors. With the exception of the IMC-41A10-treated NCI-H292 tumor 3, none of the IMC-41A10-treated tumors exhibited higher phosphorylated MAPK levels than the highest control IgG-treated tumors, a finding which also shows that IMC-41A10 is devoid of agonist activity. Taken together, these data show that treatment of tumor xenografts with IMC-41A10 led to a significant inhibition of tumor growth via inhibition of RON-dependent signaling in tumor cells.

Discussion

A substantial body of evidence exists to support a functional role for c-MET in human cancer (2). In addition, several c-MET receptor antagonists have shown antitumor activity in animal models, thereby implicating c-MET as a potential target for therapeutic intervention (2). In comparison with c-MET, RON has not been as extensively studied. Within the last few years, however, data have accumulated to suggest that not only is RON expressed in several cancers but it also may play a functional role in tumor formation.

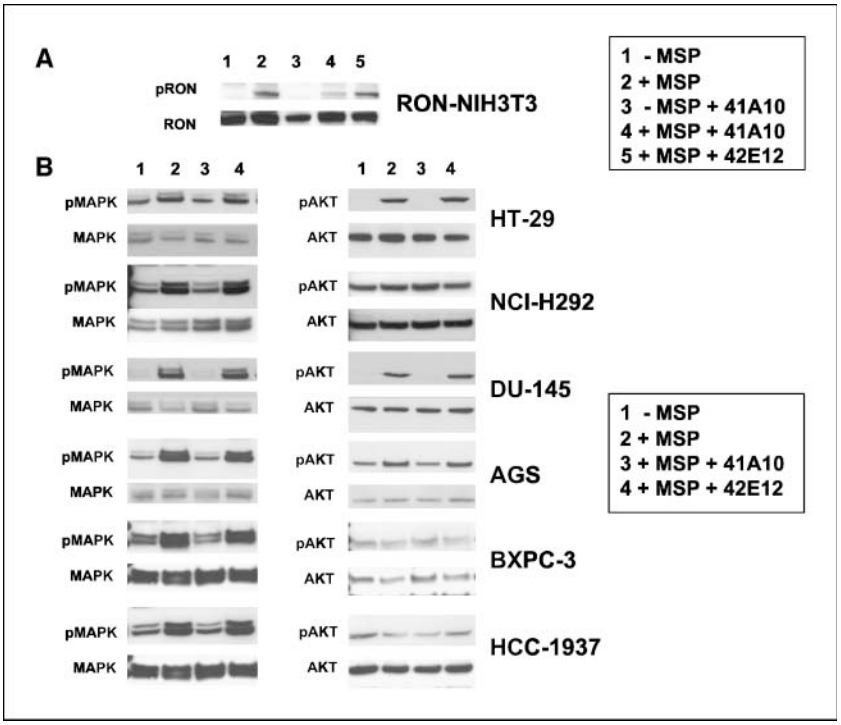

Figure 3. Inhibition of MSP-dependent receptor and MAPK phosphorylation. *A,* effect of IMC-41A10 on MSP-induced phosphorylation of RON. RON-NIH3T3 cells were serum starved (*lane 1*) and stimulated with MSP (*lanes 2, 4*, and *5*). *Lanes 3* and *4,* effect of adding IMC-41A10 in the absence and presence of MSP, respectively. *Lane 5,* effect of adding IMC-42E12, an antibody that binds to RON but does not block MSP binding, in the presence of MSP. *B,* effect of IMC-41A10 on MSP-induced phosphorylation of MAPK in cell lines representing six types of cancer. These lines were serum starved (*lane 1*) and stimulated with MSP (*lane 2*). *Lanes 3* and *4,* effect of adding IMC-41A10 in comparison with IMC-42E12, respectively.

Although RON antagonists have been reported (41–44), to our knowledge, none have been tested for antitumor activity to validate RON as a potential cancer target. Consequently, we developed IMC-41A10, a fully human IgG1 antibody that binds to human RON with high affinity (ED_{50} = 0.15 nmol/L) and blocks interaction with its ligand, MSP (IC_{50} = 2 nmol/L). IMC-41A10 does not bind to c-MET and possesses no agonist activity.

Whereas other neutralizing antibodies have been reported for RON (42), IMC-41A10 represents the first RON antibody to show antitumor activity. As a single agent, IMC-41A10 showed 50% to 60% inhibition of established tumor growth in three s.c. xenograft models using HT-29 colon, NCI-H292 lung, and BXPC-3 pancreatic cancer cells. We hypothesize that the reason IMC-41A10 treatment alone did not lead to tumor growth stabilization or regression in these three cell lines is because pathways in addition to RON are required for their tumorigenicity. Consistent with this notion is the fact that when IMC-41A10 treatment was given in combination with Erbitux (an anti-EGFR antibody) in BXPC-3 xenografts, tumor regression was observed in 5 of 12 mice. In contrast, although IMC-41A10 and Erbitux significantly inhibited BXPC-3 tumor growth, neither antibody, on its own, led to tumor growth stabilization or regression. In the future, it will be important to determine whether enhanced tumor inhibition will result following combination treatment with other antibodies or targeted therapies as well

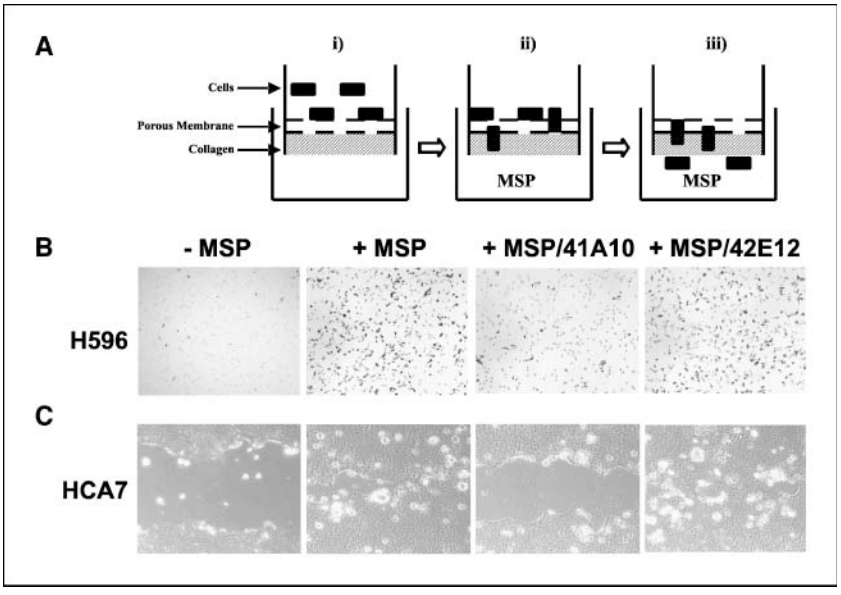

Figure 4. Ability of IMC-41A10 to inhibit cell migration. *A,* schematic of cell migration assay. *i,* cells are placed in the upper chamber of a cell culture insert and lowered into a well of a 24-well plate containing serum-free medium. The cell culture insert contains a porous membrane with collagen coated on its underside. After 24 hours, fresh serum-free medium containing MSP ± antibody is added to the lower chamber (*ii*) and cells migrate through the porous membrane and collagen and adhere to the underside of the collagen (*iii*). *B,* H&E staining of H596 lung cancer cells that have adhered to and migrated through to the underside of the collagen in the presence of IMC-41A10 and IMC-42E12, an antibody that binds to RON but does not block MSP binding. *C, in vitro* wound healing assay. A scratch was made in a monolayer of HCA7 colon cancer cells. IMC-41A10 was added to determine whether it could inhibit the ability of MSP to induce the migration of cells to fill the wound.

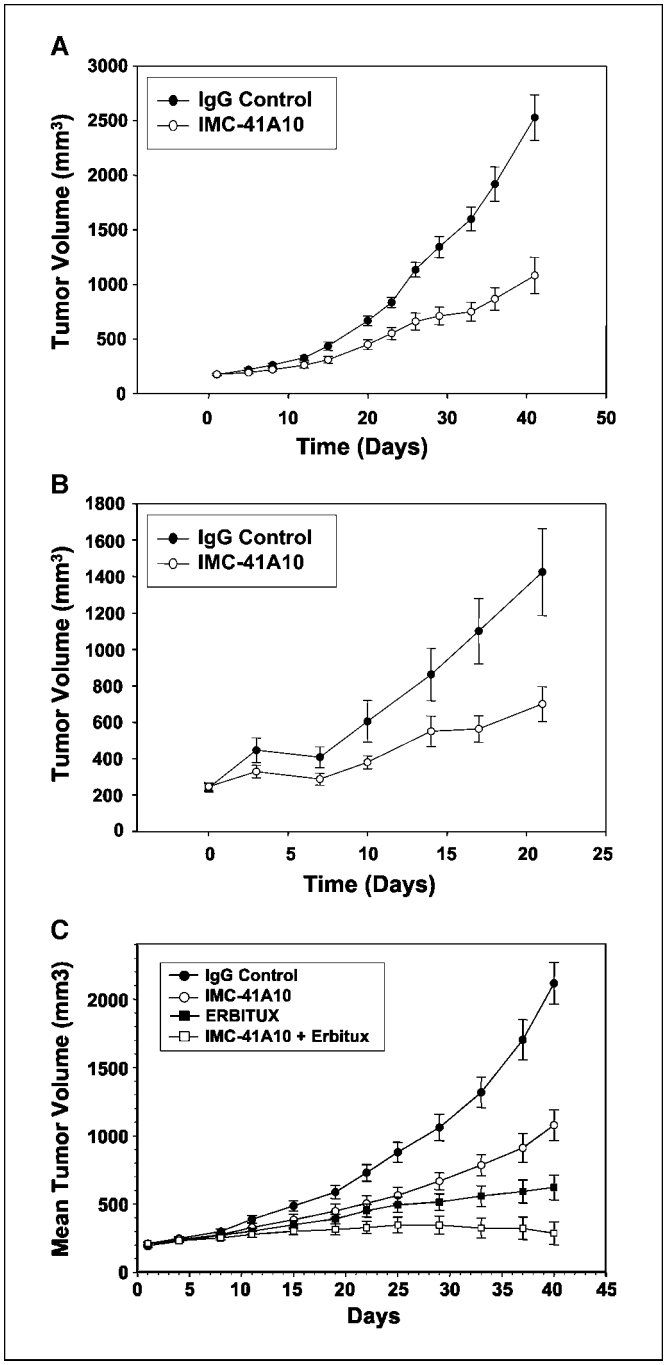

Figure 5. IMC-41A10 inhibits the growth of tumor xenografts in nude mice. HT-29 colon (*A*), NCI-H292 lung (*B*), and BXPC-3 pancreatic (*C*) cancer cells were injected s.c. into nude mice and allowed to grow to ~250 mm^3. Groups of 12 mice each were treated i.p. with 40 mg/kg of control human IgG or IMC-41A10 every 3 days. BXPC-3 xenograft tumor-bearing mice were also i.p. treated with Erbitux or the combination of Erbitux and IMC-41A10, each administered at 40 mg/kg every 3 days. Tumor size was measured with a caliper at regular intervals. *Bars,* SE. Statistical significance was determined by Student's *t* test.

as with various forms of chemotherapy and radiation. Testing the efficacy of IMC-41A10 in other subcutaneous as well as orthotopic tumor xenograft models will also be of interest.

Interestingly, IMC-41A10 inhibition of RON activity and tumorigenicity in HT-29 cells is consistent with the work of Xu et al. (31) who showed that repression of RON expression in HT-29 cells by RNA interference caused a decrease in cell proliferation and an increase in apoptosis. HT-29 cells have been shown to express constitutively active splice variants of RON with small deletions in the extracellular portion that possess enhanced oncogenic potential (26–28). Whereas we have not determined whether IMC-41A10 can interact with these constitutively active oncogenic RON variants, it is noteworthy that IMC-41A10 showed strong antitumor activity in HT-29 cells that express wild-type RON in addition to the splice variants.

Despite the fact that IMC-41A10 cross-reacts with murine RON (data not shown), no adverse effects were noted during treatment of tumor-bearing mice in this study. Thus, it seems that toxicity is not associated with inhibition of murine RON activity. This is an important finding given the phenotype of RON knockout mice and the role that RON is thought to play in normal inflammatory cells as a potential negative regulator of inflammation (8, 9).

To investigate the antitumor activity of IMC-41A10, we considered ligand-dependent and -independent mechanisms. With regard to the former, we evaluated whether IMC-41A10 could modulate MSP-dependent MAPK and AKT activation as well as cell migration.

Like HGF, it is well established that MSP (HGF-like protein) affects cell migration/invasion. Moreover, it is believed that cancer cells expressing c-MET or RON are prone to tissue invasion and metastasis (2, 3, 25). Using two *in vitro* cell migration assays, we showed IMC-41A10 to be a potent inhibitor of MSP-induced cell migration in H596 lung and HCA7 colon cancer cells. In the future, it will be of interest to determine whether IMC-41A10 will show efficacy in *in vivo* tumor metastasis models using these and other cell lines.

MAPK and AKT are known to be key downstream effector molecules governing a variety of cellular pathways respectively associated with cell growth and survival. Because MAPK and AKT have been shown to be modulated by RON receptor signaling (12), we were keen to discover whether IMC-41A10 could inhibit their phosphorylation and subsequent activation. We found IMC-41A10 to be a potent inhibitor of MSP-induced phosphorylation of MAPK *in vitro* in HT-29 cells as well as in cultured NCI-H292, DU145, AGS, BXPC-3, and HCC-1937 cells, which represent lung, prostate, gastric, pancreatic, and breast cancer, respectively. IMC-41A10 also proved to be a potent inhibitor of AKT phosphorylation in HT-29, DU145, and AGS cells. In HT-29 and NCI-H292 tumor xenografts treated with IMC-41A10 for 24 and 72 hours, respectively, we observed a 35% and 28% inhibition of MAPK phosphorylation following a single treatment. Because IMC-41A10 treatment of HT-29 and NCI-H292 tumor xenografts occurred for several weeks, it is reasonable to assume that the cumulative effect of IMC-41A10 treatment on MAPK activity would be to significantly and negatively affect tumor growth. Because HT-29 and NCI-H292 cells do not produce MSP (Supplementary Fig. S4) but are sensitive to MSP stimulation *in vitro*, our data suggest not only that *in vivo* activation of MAPK in these cell lines is mediated by paracrine stimulation of the RON receptor with murine MSP but also that IMC-41A10 effectively inhibits the murine MSP-RON interaction. Taken together, the inhibitory effects of IMC-41A10 on MAPK and AKT phosphorylation would suggest not only a negative effect on cell growth and survival but may also be predictive of the antitumor potential of IMC-41A10 treatment in cancer cell lines where it modulates phosphorylation of MAPK and AKT. With respect to MSP-independent mechanisms of tumor inhibition, we did experiments to test whether IMC-41A10 treatment led to (*a*)

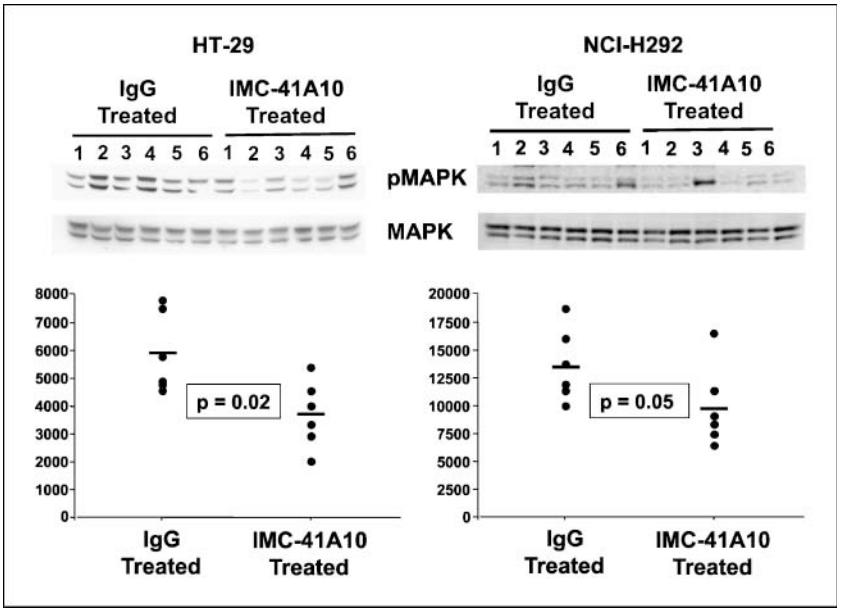

Figure 6. IMC-41A10 inhibits phosphorylation of MAPK in HT-29 and NCI-H292 tumor xenografts. HT-29 and NCI-H292 cells were s.c. injected into 24 nude mice and allowed to reach ~300 mm^3. For each cell line, six mice were treated with IMC-41A10 and six with control IgG. Twenty-four hours (HT-29) and 72 hours (NCI-H292) after a single injection with antibody at a dose of 40 mg/kg, tumors were excised and lysates prepared for Western blot analysis to detect MAPK and phosphorylated MAPK levels. Densitometric values for total MAPK bands were normalized to 20,000 and, in turn, the densitometric values of the phosphorylated MAPK bands were proportionately adjusted. The adjusted phosphorylated MAPK values for IMC-41A10-treated mice were averaged and compared with those of the control IgG-treated mice. Statistical significance between the two groups was determined by Student's *t* test.

RON receptor down-regulation (Supplementary Fig. S5*A* and *B*); (*b*) repression of vascular endothelial growth factor secretion (Supplementary Fig. S6*A*); (*c*) induction of apoptosis (Supplementary Fig. S6*B*); and (*d*) induction of complement-dependent cytotoxic or antibody-dependent cell-mediated cytotoxic activity (Supplementary Fig. S7*A* and *B*). Whereas results from these experiments were conclusive, they were also negative and did not suggest an MSP-independent mechanism of action for the antitumor activity of IMC-41A10. With respect to the inability of IMC-41A10 to elicit complement-dependent cytotoxic and antibody-dependent cell-mediated cytotoxic activities on cell lines tested, we emphasize that it is possible that IMC-41A10 (a human IgG1 antibody) could elicit such activity *in vivo*. Furthermore, we stress that other MSP-independent mechanisms may contribute to the antitumor efficacy of IMC-41A10 but await further experimentation.

Whereas some reports exist that provide evidence for RON expression in human tumors, the number of patients was not always sufficient and methods used to examine expression were varied. In this report, we conducted an extensive systematic analysis of RON expression in ~100 cancer cell lines representing 10 cancer types and in 6 different tumor types using commercial tumor tissue arrays harboring nearly 300 individual tumor samples. RON was expressed in approximately half of the cell lines and was expressed by at least one cell line per cancer type with the exception of the leukemic and renal cancer cell lines tested. With respect to the tumor tissue array results, RON was well expressed in every cancer type (breast, 100%; lung, 93%; prostate, 92%; gastric, 73%; pancreas, 69%; and colon, 65%). We observed no significant correlation between the extent of RON expression and the stage or severity of disease. These results make a significant contribution to the expression profile of RON in a variety of tumor tissues and cancer cell lines.

In conclusion, our data show that not only is RON well expressed in several cancers but it is also an "inhibitable" target that contributes to tumorigenesis. Our findings also underscore the potential of using an antibody to antagonize RON activity for the treatment of human cancers such as colon, lung, pancreas, and probably other cancers.

Acknowledgments

Received 1/24/2006; revised 6/7/2006; accepted 7/12/2006.

The costs of publication of this article were defrayed in part by the payment of page charges. This article must therefore be hereby marked *advertisement* in accordance with 18 U.S.C. Section 1734 solely to indicate this fact.

We thank Cellestan for pathologic analyses of our tumor tissue array data; Chris Damoci, Deevi Dhanvanthri, and Jim Tonra for animal work; and Anthony Kayas, Mary Amasia, Xenia Jimenez, and Dave Sargent for assistance with antibody production, purification, and characterization studies. Dedication: ILU-MdLSP-RIP.

References

1. Ronsin C, Muscatelli F, Mattei MG, Breathnach R. A novel putative receptor protein tyrosine kinase of the met family. Oncogene 1993;8:1195–202.
2. Christensen JG, Burrows J, Salgia R. c-Met as a target for human cancer and characterization of inhibitors for therapeutic intervention. Cancer Lett 2005;225:1–26.
3. Camp ER, Liu W, Fan F, Yang A, Somcio R, Ellis LM. RON, a tyrosine kinase receptor involved in tumor progression and metastasis. Ann Surg Oncol 2005;12:273–81.
4. Leonard EJ, Danilkovitch A. Macrophage stimulating protein. Adv Cancer Res 2000;77:139–67.
5. Chen YQ, Fisher JH, Wang MH. Activation of the RON receptor tyrosine kinase inhibits inducible nitric oxide synthase (iNOS) expression by murine peritoneal exudate macrophages: phosphatidylinositol-3 kinase is required for RON-mediated inhibition of iNOS expression. J Immunol 1998;161:4950–9.
6. Wang MH, Fung HL, Chen YQ. Regulation of the RON receptor tyrosine kinase expression in macrophages: blocking the RON gene transcription by endotoxin-induced nitric oxide. J Immunol 2000;164:3815–21.
7. Zhou YQ, Chen YQ, Fisher JH, Wang MH. Activation of the RON receptor tyrosine kinase by macrophage-stimulating protein inhibits inducible cyclooxygenase-2 expression in murine macrophages. J Biol Chem 2002; 277:38104–10.
8. Leonis MA, Toney-Earley K, Degen SJ, Waltz SE. Deletion of the Ron receptor tyrosine kinase domain in mice provides protection from endotoxin-induced acute liver failure. Hepatology 2002;36:1053–60.
9. Wang MH, Zhou YQ, Chen YQ. Macrophage-stimulating protein and RON receptor tyrosine kinase: potential regulators of macrophage inflammatory activities. Scand J Immunol 2002;56:545–53.
10. Chen YQ, Zhou YQ, Wang MH. Activation of the RON receptor tyrosine kinase protects murine macrophages from apoptotic death induced by bacterial lipopolysaccharide. J Leukoc Biol 2002;71:359–66.
11. Wang MH, Dlugosz AA, Sun Y, Suda T, Skeel A, Leonard EJ. Macrophage-stimulating protein induces

proliferation and migration of murine keratinocytes. Exp Cell Res 1996;226:39–46.
12. Danilkovitch-Miagkova A. Oncogenic signaling pathways activated by RON receptor tyrosine kinase. Curr Cancer Drug Targets 2003;3:31–40.
13. Chen YQ, Zhou YQ, Angeloni D, Kurtz AL, Qiang XZ, Wang MH. Overexpression and activation of the RON receptor tyrosine kinase in a panel of human colorectal carcinoma cell lines. Exp Cell Res 2000;261:229–38.
14. Willett CG, Wang MH, Emanuel RL, et al. Macrophage-stimulating protein and its receptor in non-small-cell lung tumors: induction of receptor tyrosine phosphorylation and cell migration. Am J Respir Cell Mol Biol 1998;18:489–96.
15. Maggiora P, Marchio S, Stella MC, et al. Overexpression of the RON gene in human breast carcinoma. Oncogene 1998;16:2927–33.
16. Lee WY, Chen HH, Chow NH, Su WC, Lin PW, Guo HR. Prognostic significance of co-expression of RON and MET receptors in node-negative breast cancer patients. Clin Cancer Res 2005;11:2222–8.
17. Okino T, Egami H, Ohmachi H, et al. Immunohistochemical analysis of distribution of RON receptor tyrosine kinase in human digestive organs. Dig Dis Sci 2001;46:424–9.
18. Maggiora P, Lorenzato A, Fracchioli S, et al. The RON and MET oncogenes are co-expressed in human ovarian carcinomas and cooperate in activating invasiveness. Exp Cell Res 2003;288:382–9.
19. Cheng HL, Liu HS, Lin YJ, et al. Co-expression of RON and MET is a prognostic indicator for patients with transitional-cell carcinoma of the bladder. Br J Cancer 2005;92:1906–14.
20. Chen Q, Seol DW, Carr B, Zarnegar R. Co-expression and regulation of Met and Ron proto-oncogenes in human hepatocellular carcinoma tissues and cell lines. Hepatology 1997;26:59–66.
21. Rampino T, Gregorini M, Soccio G, et al. The Ron proto-oncogene product is a phenotypic marker of renal oncocytoma. Am J Surg Pathol 2003;27:779–85.
22. Patton KT, Tretiakova MS, Yao JL, et al. Expression of RON proto-oncogene in renal oncocytoma and chromophobe renal cell carcinoma. Am J Surg Pathol 2004; 28:1045–50.
23. Peace BE, Hill KJ, Degen SJ, Waltz SE. Cross-talk between the receptor tyrosine kinases Ron and epidermal growth factor receptor. Exp Cell Res 2003;289: 317–25.
24. Follenzi A, Bakovic S, Gual P, Stella MC, Longati P, Comoglio PM. Cross-talk between the proto-oncogenes Met and Ron. Oncogene 2000;19:3041–9.
25. Tamagnone L, Comoglio PM. Control of invasive growth by hepatocyte growth factor (HGF) and related scatter factors. Cytokine Growth Factor Rev 1997;8: 129–42.
26. Wang MH, Wang D, Chen YQ. Oncogenic and invasive potentials of human macrophage-stimulating protein receptor, the RON receptor tyrosine kinase. Carcinogenesis 2003;24:1291–300.
27. Zhou YQ, He C, Chen YQ, Wang D, Wang MH. Altered expression of the RON receptor tyrosine kinase in primary human colorectal adenocarcinomas: generation of different splicing RON variants and their oncogenic potential. Oncogene 2003;22:186–97.
28. Peace BE, Hughes MJ, Degen SJ, Waltz SE. Point mutations and overexpression of Ron induce transformation, tumor formation, and metastasis. Oncogene 2001;20:6142–51.
29. Chen YQ, Zhou YQ, Fisher JH, Wang MH. Targeted expression of the receptor tyrosine kinase RON in distal lung epithelial cells results in multiple tumor formation: oncogenic potential of RON *in vivo*. Oncogene 2002;21: 6382–6.
30. Chen YQ, Zhou YQ, Fu LH, Wang D, Wang MH. Multiple pulmonary adenomas in the lung of transgenic mice overexpressing the RON receptor tyrosine kinase, Recepteur d'origine nantais. Carcinogenesis 2002;23: 1811–9.
31. Xu XM, Wang D, Shen Q, Chen YQ, Wang MH. RNA-mediated gene silencing of the RON receptor tyrosine kinase alters oncogenic phenotypes of human colorectal carcinoma cells. Oncogene 2004;23:8464–74.
32. Santoro MM, Collesi C, Grisendi S, Gaudino G, Comoglio PM. Constitutive activation of the RON gene promotes invasive growth but not transformation. Mol Cell Biol 1996;16:7072–83.
33. Wang MH, Kurtz AL, Chen Y. Identification of a novel splicing product of the RON receptor tyrosine kinase in human colorectal carcinoma cells. Carcinogenesis 2000; 21:1507–12.
34. Okino T, Egami H, Ohmachi H, et al. Presence of RON receptor tyrosine kinase and its splicing variant in malignant and non-malignant human colonic mucosa. Int J Oncol 1999;15:709–14.
35. Collesi C, Santoro MM, Gaudino G, Comoglio PM. A splicing variant of the RON transcript induces constitutive tyrosine kinase activity and an invasive phenotype. Mol Cell Biol 1996;16:5518–26.
36. Peace BE, Toney-Earley K, Collins MH, Waltz SE. Ron receptor signaling augments mammary tumor formation and metastasis in a murine model of breast cancer. Cancer Res 2005;65:1285–93.
37. Chan EL, Peace BE, Collins MH, Toney-Earley K, Waltz SE. Ron tyrosine kinase receptor regulates papilloma growth and malignant conversion in a murine model of skin carcinogenesis. Oncogene 2005; 24:479–88.
38. Burtrum D, Zhu Z, Lu D, et al. A fully human monoclonal antibody to the insulin-like growth factor I receptor blocks ligand-dependent signaling and inhibits human tumor growth *in vivo*. Cancer Res 2003;63:8912–21.
39. Hoet RM, Cohen EH, Kent RB, et al. Generation of high-affinity human antibodies by combining donor-derived and synthetic complementarity-determining-region diversity. Nat Biotechnol 2005;23:344–8.
40. Lu D, Jimenez X, Zhang H, Bohlen P, Witte L, Zhu Z. Selection of high affinity human neutralizing antibodies to VEGFR2 from a large antibody phage display library for antiangiogenesis therapy. Int J Cancer 2002;97:393–9.
41. Bardelli A, Longati P, Williams TA, Benvenuti S, Comoglio PM. A peptide representing the carboxyl-terminal tail of the met receptor inhibits kinase activity and invasive growth. J Biol Chem 1999;274:29274–81.
42. Montero-Julian FA, Dauny I, Flavetta S, et al. Characterization of two monoclonal antibodies against the RON tyrosine kinase receptor. Hybridoma 1998;17: 541–51.
43. Angeloni D, Danilkovitch-Miagkova A, Miagkov A, Leonard EJ, Lerman MI. The soluble sema domain of the RON receptor inhibits macrophage-stimulating protein-induced receptor activation. J Biol Chem 2004; 279:3726–32.
44. Matzke A, Herrlich P, Ponta H, Orian-Rousseau V. A five-amino-acid peptide blocks Met- and Ron-dependent cell migration. Cancer Res 2005;65:6105–10.

Instructions for Submitting
More About File Formats
More About MS Status
Copyright Form

My Manuscripts

Sort by MS Number Sort ▲ Sort ▼

Sorted ▼ by **MS Number**

[Mammary-Specific Ron Receptor Overexpression Induces Highly Metastatic Mammary Tumors Associated With β-catenin Activation]
Journal Name: Cancer Research
MS # CAN-06-2473 Version 1
MS Status: **Accept Pending Revision** View Decision Letter Resubmit

[Ron receptor signaling augments mammary tumor formation and metastasis in a murine model of breast cancer]
Journal Name: Cancer Research
MS # CAN-03-3580 Version 3
MS Status: **MS Published** View Decision Letter

Mammary-Specific Ron Receptor Overexpression Induces Highly Metastatic Mammary Tumors Associated With β-catenin Activation

Glendon M. Zinser[1], Mike A. Leonis[2], Kenya Toney[1], Peterson Pathrose[1], Megan Thobe[1], Sarah A. Kader[1], Belinda E. Peace[1], Shirelyn R. Beauman[1], Margaret H. Collins[2] and Susan E. Waltz[1*]

Departments of Surgery[1] and Pediatrics[2], University of Cincinnati College of Medicine and Cincinnati Children's Hospital Medical Center, Cincinnati, OH 45267-0558. USA

*Address Correspondence to:
Susan E. Waltz, Ph.D.
Department of Surgery
Division of Research
University of Cincinnati College of Medicine
231 Albert Sabin Way
Cincinnati, OH 45267-0558
Phone: 513-558-8675
Fax: 513-558-8677
e-mail: susan.waltz@uc.edu

Running Title: Ron Overexpression Induces Mammary Tumorigenesis

Key Words: Ron receptor, Met receptor, b-catenin, mammary tumorigenesis, metastasis

Abstract

Activated growth factor receptor tyrosine kinases play pivotal roles in a variety of human cancers, including breast cancer. Ron, a member of the Met receptor tyrosine kinase protooncogene family, is overexpressed or constitutively active in 50% of human breast cancers. To define the significance of Ron overexpression and activation in vivo, we generated transgenic mice that overexpress a wild type or constitutively active Ron receptor in the mammary epithelium. In these animals, Ron expression is significantly elevated in mammary glands and leads to a hyperplastic phenotype by 12 weeks of age. Ron overexpression is sufficient to induce mammary transformation in all transgenic animals and is associated with a high degree of metastasis, with metastatic foci detected in liver and lungs of over 86% of all transgenic animals. Furthermore, we show that Ron overexpression leads to receptor phosphorylation and is associated with elevated levels of tyrosine phosphorylated β-catenin and the upregulation of genes, including cyclin D1 and c-myc, which are associated with poor prognosis in patients with human breast cancers. These studies suggest that Ron overexpression may be a causative factor in breast tumorigenesis and provides a model to dissect the mechanism by which the Ron induces transformation and metastasis.

Introduction

Overexpression or increased activation of receptor tyrosine kinases has been associated with many malignant human cancers, including breast cancer. Breast cancer prognosis has been associated with abnormal receptor tyrosine kinase expression due to gene amplification, protein overexpression, or abnormal transcriptional regulation (1-3). Moreover, a number of studies have reported that protein kinase activity is higher in most malignant human cancers compared to normal tissue or in benign tumors (4-7). Recently, the Ron receptor tyrosine kinase has been shown to be overexpressed and constitutively active in about 50% of primary breast cancer cases (8), and increased expression of Ron receptor strongly correlates with the more aggressive phenotype observed in node-negative breast tumors (9). These findings raise the question of whether overexpression or activation of the Ron receptor is a driving force in mammary gland tumorigenesis *in vivo*.

The Ron receptor is a member of a distinct subfamily of receptor tyrosine kinases that includes the Met proto-oncogene. In its mature form, Ron exists as a heterodimer composed of a 35 kDa extracellular α chain and a 150 kDa transmembrane-spanning β chain with intrinsic tyrosine kinase activity. Upon binding its ligand, hepatocyte growth factor-like protein (HGFL), Ron becomes phosphorylated at key intracellular tyrosine residues that provide docking sites for downstream signaling adapter molecules (10-14). Ligand-stimulated Ron triggers activation of a number of signaling pathways, including PI3K/AKT, MAPK, JNK, and β-catenin, which participate in cell proliferation, differentiation and migration (11-14). Ron activation induces "invasive growth" of transformed cells, leading to cell-cell dissociation (scattering), cellular proliferation, cell motility, morphological changes and increased tumorigenic capacity (13-16).

A number of human neoplastic syndromes are associated with activating point mutations in a highly conserved region of the Met tyrosine kinase domain; *in vitro*, these mutations lead to the accumulation and recruitment of the β-catenin signaling pathway (17, 18). The oncogenic potential of

Ron receptor gain-of-function has been assessed *in vitro* by overexpressing either wild type Ron or analogous mutant forms of Ron in transformed cell lines. Our laboratory and others have shown that overexpression of wild type Ron or constitutively active mutant forms of Ron give rise to increased tumorigenic properties of transformed cell lines, which may be mediated in part by activation of the β-catenin signaling cascade (19, 20).

Whereas these studies suggest that elevated expression of wild type Ron can transform epithelial cells *in vitro*, the potential for Ron overexpression to induce mammary tumorigenesis *in vivo* remains to be established. To investigate the significance of Ron overexpression in the mammary gland, we created transgenic mice overexpressing either wild type Ron (WT-Ron) or a constitutively active form of Ron (MT-Ron) in the mammary epithelium under the control of the mouse mammary tumor virus (MMTV) promoter. This approach allowed us to directly assess the impact of Ron receptor overexpression on mammary tumorigenesis and metastasis.

These studies show that Ron overexpression or constitutive activation within the mammary gland is sufficient to induce mammary tumors at a high incidence and containing aggressive metastatic potential. Our work suggests that Ron receptor signaling not only plays a vital role in mammary gland tumor formation, but also serves as a critical regulator of the complex biological processes utilized for epithelial cell metastasis. Most importantly, these studies provide an *in vivo* animal model that recapitulates the aggressive phenotype observed in Ron overexpressing human breast tumors.

Materials and Methods

Cloning and construction of the Ron transgenes: Wild type and constitutively-active murine Ron minigenes were constructed utilizing 5' genomic DNA and 3' cDNA fragments of the mouse (m) Ron gene (accession numbers U65949 and X74736, respectively; see Figure 1) (19, 21, 22). A 3.2 kb SpeI/EcoRI fragment of mRon genomic DNA encompassing exon 1 and half of intron 1 was cloned into pBluescript. Subsequently, a 3.2 kb EcoRI mRon genomic DNA fragment encompassing exons 2-6 was cloned into EcoRI-digested of this plasmid. A 2.8 kb AgeI/XhoI fragment of mRon cDNA encoding exons 4-19 was directionally cloned into AgeI/XhoI-digested plasmid, giving rise to a vector harboring a full-length wild type mRon minigene. For the constitutively active Ron construct, an analogous 2.8 kb AgeI/XhoI fragment of a mRon cDNA harboring a methionine-to-threonine point mutation at amino acid 1231 of the mRon cDNA sequence (19) was generated.

A 2.3 kb BamHI DNA cassette harboring the mouse mammary tumor virus (MMTV) promoter was excised from vector pA9 (23), and cloned into BamHI-digested pIND (Invitrogen), giving rise to MMTV-pIND. The 8.4 kb NotI fragments containing the wild type and ΔM1231T mRon minigenes were then cloned into the NotI site of MMTV-pIND, giving rise to a vector harboring the MMTV promoter 5' to the respective mRon minigene constructs. Excision of these plasmids with PmeI yielded 10.806 kb MMTV promoter-driven mRon DNA constructs (see Figure 1).

Generation and identification of transgenic animals: The Ron minigene constructs were injected into fertilized eggs from FVB/N mice. Positive founders were crossed with wild type FVB/N mice (Taconic Laboratory, Germantown, NY) to generate the F_1 offspring. F_1 positive mice were subsequently crossed with wild type littermates to generate offspring utilized in the analyses. Genotype analysis of the transgenic mice was determined by PCR and Southern analyses. For PCR analyses, primers (5'-TGGGTGGTGAGGTCTGCCAACATGAGCTCC-3') and (5'-

CCGTCTTCGGGAGTTAAAGATCAGGGCAAC-3') were used and produced a 251bp fragment corresponding to the Ron minigene and a 331bp fragment corresponding to the endogenous Ron sequence. Transgenic transmission was furthered confirmed by Southern analysis using a 708bp probe. For Southern analysis, DNA was digested with BamH1 and the Southern membranes were probed with a PCR generated fragment (5'- TCCCCAACAACACTCTCTGACATCA-3' and 5'-ACAAAGGACCTGCAGCCTGAGGTCA-3'). For Southern analyses, a genomic band of 4.7kb is generated while a band of 3.7kb is obtained from the transgene insertion. Copy number was determined by comparison to the endogenous allele. All animal procedures were approved by the University of Cincinnati Animal Care and Use Committee.

RNA isolation and Northern Analysis: Total RNA was isolated from tissues using Trizol (Invitrogen, Carlsbad, CA). RNA containing membranes were hybridized at 68°C for 24 hours with a mouse Ron cDNA. Membranes were exposed to a PhosphorImager (Molecular Dynamics STORM 860 PhosphorImager system, Piscataway, NJ). The membrane was reprobed with a 213bp GAPDH PCR fragment (5' -GCTCCTCTCGCCAAGGTTATTC-3' and 5' -GCTCTGGGATGACTTTGCCTACAG-3' accession number MMU09964).

Protein Isolation and Western Analysis: Tissues were homogenized in protein lysis buffer [50mM Tris, pH 7.4, 0.5% Triton X-100, 0.5% IGEPAL, 150mM NaCl, 2mM EDTA] containing protease inhibitor (Complete®, mini, EDTA-free, Roche Diagnostics, Indianapolis, IN) and 1mM Na_3VO_4. Proteins were separated by SDS-PAGE and transfered to Immobilon P membranes (Millipore, Billerica, MA). After transfer, the membranes were probed with a rabbit polyclonal anti-Ron antibody (1:500) (Santa Cruz Biotechnology, Inc., Santa Cruz, CA). Specific binding was detected using an anti-rabbit alkaline phosphatase secondary antibody. The membrane was developed using electro-

chemifluorescence (ECF) Western detection reagent (Amersham Biosciences, Piscataway, NJ) and images were captured by the AlphaInnotech gel documentation system (San Leandro, CA).

The membrane was stripped and re-probed sequentially with the following antibodies: anti-pRon (Biosource International, Camarillo, CA), anti- β-catenin (Sigma Aldrich, St. Louis, MO), anti-cyclin D1 (Santa Cruz Biotechnology, Inc., Santa Cruz, CA), anti-MAPK (Upstate Cell Signaling Solutions, Lake Placid, NY), anti-phospho- p44/42 Map Kinase (Thr202/Tyr 204) (Cell Signaling Technology, Danvers, MA), anti-c-Myc (Neomarkers, Fremont, CA), and anti-actin antibody C4.

For co-immunoprecipitation experiments, total tissue lysates (1mg) were incubated with 5μg of the indicated primary antibodies followed by incubation with protein G-agarose overnight at 4°C. The immunocomplexes were washed 3x and bound proteins were eluted by boiling in SDS sample buffer and subjected to SDS-PAGE. Western membranes were then probed with anti-Ron, anti-β-catenin, anti-pRon, and anti-p-tyrosine (4G10, Upstate Cell Signaling Solutions, Lake Placid, NY) primary antibodies as noted above.

Electromobility shift assays were performed on whole cell lysates from non-transgenic and transgenic mammary tissue. Double stranded oligonucleotides containing the core consensus TCF/Lymphoid Enhancement Factor (LEF) binding site, 5' - CTC TGC CGG GCT TTG ATC TTT GCT TAA CAA CA - 3' and 5' – TGT TGT TAA GCA AAG ATC AAA GCC CGG CAG AG – 3', were labeled by end-labeling reactions using [^{32}P]dATP. Approximately 1.75pmol of labeled probe was added to 25μg of lysate and incubated for 30 minutes. Protein-DNA complexes were resolved through a non-denaturing 4% polyacrylamide gel and exposed to a phosphoimager.

Tumor Development Curves: Animals were examined weekly for mammary tumor development by palpation for up to 400 days, and tumor incidence was plotted against time. Data on tumor development was subjected to Kaplan-Meier analysis using GraphPad Prism for Windows (GraphPad Software, San Diego, CA). All mice upon excessive tumor burden were euthanized by CO_2

asphyxiation, and mammary glands, tumors, liver and lungs were removed for histological examination.

Tissue Histology and Immunohistochemistry: For whole mount analysis, mammary glands were fixed in Carnoy's fixative and stained overnight in Carmine Alum. Samples were dehydrated, cleared in xylene, mounted, and examined on a stereoscope equipped with an Axiovert digital camera.

Tissues were processed as indicated previously (19). Four μm sections of lung and liver tissue were taken at 40 to 200 μm intervals, respectively, along the entire tissue to obtain full coverage of this organ. Sections were stained with hematoxylin-eosin for routine histological examination for metastatic tumor foci. Staining for Ron protein in lung metastasis sections was performed on formalin-fixed, paraffin embedded sections. Sections were stained with a rabbit polyclonal antibody specific to Ron (Santa Cruz Biotechnology, Inc., Santa Cruz, CA). The slides were developed using a biotinylated secondary antibody incubated with Vectastain ABC kit (Vector Laboratories, Burlingame, CA) that was further amplified with a Vector Alkaline Phosphatase substrate kit (Vector Laboratories, Burlingame, CA).

Results

Generation of transgenic mice expressing wild type and constitutively active Ron in the mammary epithelium.

To determine whether Ron is sufficient for the oncogenic effects observed in human patients, we generated two new murine models to mimic Ron overexpression and activation observed in human breast cancer specimens. In one model we generated a minigene construct containing a wild type Ron expression cassette (Figure 1A). In the constitutively active Ron transgene, a point mutation was generated analogous to the mutation observed in human cancers in the receptor tyrosine kinases Met, Kit, and Ret (24-28). The ΔM1231T (MT-Ron) point mutation refers to the substitution of a threonine for a methionine at residue 1231 (open arrow, Figure 1A) and has been shown to cause constitutive activation of the receptor, leading to transformation *in vitro* and tumorigenicity *in vivo* (19). Each construct was placed under the transcriptional control of the MMTV promoter (Figure 1A). The expression cassettes were excised from the vector and were injected into fertilized eggs from FVB/N mice. Positive founders were crossed with wild type FVB/N mice to produce F_1 offspring. Based on Southern analysis of tail biopsies, we identified four transgenic lines for the MMTV-Ron (WT-Ron [R3, R4, R6, R7]) construct, and two MMTV-Ron (ΔM1231T) (MT-Ron [M9, M10]) transgenic lines that were studied further. The copy number of each transgenic line was determined by comparing the intensity of the transgenic allele to that of the endogenous allele and varied between 1 to 5 copies per line. All founder animals transmitted the transgene to their progeny in Mendelian fashion as determined by PCR with primers designed to detect endogenous Ron and the transgenic copy of the Ron minigene constructs (data not shown).

To test the tissue distribution of the transgene, we isolated mammary gland and other tissues from non-transgenic (Tg-) and transgenic (Tg+) mice. Protein extracts were generated from each tissue and were analyzed for the amount of Ron expression. Ron expression was found to be very high in the Tg+ mammary gland compared to the Tg- mammary gland. In addition, we also detected

transgene expression in the lacrimal gland. In contrast, no transgene expression was found in any of the other tissues that were isolated (Figure 1B). Thus, the transgenes were highly and selectively expressed within mammary tissue and to a limited extent in the lacrimal gland.

During propagation of the mice, lacrimal gland swelling was apparent in a number of transgene positive mice. To analyze the effect of Ron overexpression within this tissue, we isolated a subset of lacrimal glands from Tg- and Tg+ mice and processed them for histological analysis. The expression of Ron in the lacrimal gland produced epithelial hyperplasia that gave rise to dilated and cystic acini (Figure 1C). However, no further progression of this phenotype was observed.

Effect of Ron overexpression on mammary gland development and transformation

To assess whether mammary-specific Ron overexpression would alter normal mammary development, we isolated mammary glands from Tg- and Tg+ 12-week-old virgin mice for wholemount and histological analysis. Normal mammary gland development is seen by whole mount analysis in glands from the Tg- mice at twelve weeks of age, displaying an abundance of secondary and tertiary branch points and thin mammary ducts that fill the mammary fat pad and show little evidence of alveolar development (Figure 2A). In contrast, mammary glands from Tg+ mice, WT-Ron and MT-Ron, display pronounced ductal ectasia with dramatic ductal thickening and regression of tertiary branches, resulting in stubby, dilated ducts, and acinar hyperplasia (Figure 2B).

Histological examination of mammary glands from 12-week-old mice illustrate the dilated ducts and multilayered epithelium found in the glands of Ron transgenic mice (Figure 2 D) compared to the glands of Tg- mice that have a well-organized columnar epithelium giving rise to an organized ductal morphology (arrowhead, Figure 2 C). In addition, secretory vacuolization was apparent in Tg+ mammary glands (arrow, Figure 2D), resembling a mammary morphology from a pregnant female. The mammary gland from Tg+ mice also contained small clusters of epithelial hyperplasia (block

arrow, Figure 2D). By four months of age, Tg+ glands have a large number of well-developed hyperplastic alveolar nodules (data not shown).

This assessment of transgenic mammary gland morphology is consistent with prior observations that this receptor family regulates events controlling branching morphogenesis (29, 30). Moreover, these data suggest that Ron overexpression is sufficient to induce ductal hyperplasia and ultimately breast tumorigenesis. To follow tumor development in these animals, weekly palpation of multiparous WT-Ron and MT-Ron Tg+ mice was performed. Tumor kinetics were plotted by monitoring tumor development as the percentage of tumor free mice versus time (Figure 3A). The non-transgenic mice did not develop mammary tumors. Given that all of the four WT-Ron transgenic lines and both of the MT transgenic lines produced similar results regardless of the integration site and copy number, the data from the WT lines were pooled and likewise, the data from the MT lines were pooled. By 189 days of age, 50% of the constitutively active MT-Ron mice had palpable mammary tumors compared to the WT-Ron transgenic mice that reached 50% tumor incidence at day 202. Although tumor latency was significantly different between transgenic lines as determined by Kaplan Meier analysis, the overall tumor incidence was similar in both transgenic lines, producing 100% tumor incidence.

The tumor morphology that developed as a result of Ron overexpression was diverse, ranging from the most prevalent form being adenocarcinoma (Figure 3B, a) with a varying degree of desmoplastic epithelial malignancy (Figure 3B, b) to a more papillary carcinoma (Figure 3B, c). The tumors that developed contained a number of mitotic figures, an increased nuclear to cytoplasmic ratio and a high degree of pleomorphism that resembles what is observed in aggressive human disease. Tumors from both transgenic lines were highly invasive, as shown by the local invasion of the underlying connective tissue stroma and musculature (arrow, Figure 3B, d).

Mammary-specific Ron overexpression leads to highly metastatic mammary tumors

The tumors that arose in WT-Ron and MT-Ron transgenic mice displayed a very aggressive phenotype. Upon microscopic evaluation, the Ron overexpressing tumor cells were locally invasive as shown by the penetration of tumor cells into the underlying connective stroma and muscle tissue in Figure 3B, d. Furthermore, distant metastatic foci were found in the lung and liver both grossly at dissection and upon histological analyses (Figure 4A). Overexpression of Ron induced metastases in a high percentage of mice with a majority of the Tg+ animals having foci in the lungs and livers (Figure 4B). The dramatic percentage of animals with metastases suggests that Ron overexpression gives rise to an aggressive mammary tumor phenotype and is similar to the aggressive nature of human breast cancers observed overexpressing Ron (9).

As indicated, many transgenic mice displayed evidence of gross metastasis as depicted in a representative lung sample (Figure 4A, a). Interestingly, many metastatic foci were observed growing within the vasculature of the lungs and liver (asterisks in Figure 4A, b, and data not shown). This data indicates that Ron overexpressing mammary cells are hematogenously disseminated, become lodged in select organs, and are capable of growing within the vessels of select target organs. In addition, metastatic cells were also seen efficiently invading into normal lung and liver parenchyma with metastatic mammary tumor cells evident among the hepatocytes of the liver (Figure 4A, c). The metastatic foci found in the lung and liver distinctly resembled the primary mammary tumor cells and displayed mitotic figures that were not observed in sections of lung or liver from control animals. To determine if these distal foci retained Ron expression, metastatic tumor sections were examined by immunohistochemistry. As illustrated in Figure 4A, d, intense Ron expression was observed in the metastatic foci.

Ron overexpression activates signaling cascades involved in cell proliferation/survival and associates with β-catenin

To ensure that the observed mammary tumors retained Ron expression, we isolated RNA and protein from Tg- and Tg+ mammary tissue to compare transgene expression within the mammary gland and in the resulting mammary tumors. In contrast to the Tg- mammary tissue in which Ron expression was undetectable, Ron mRNA expression was observed in the hyperplastic mammary ducts in all Tg+ lines and noticeably higher expression in palpable mammary tumor tissue (Figure 5A). Protein isolated from the palpable tumor samples showed a similar pattern of Ron expression by Western analyses, with a dramatic increase in Ron expression in all tumor samples compared to the Tg- tissue (Figure 5B). To determine if Ron overexpression in this transgenic model results in constitutive receptor activation, an antibody that recognizes the phosphorylated active form of Ron was utilized. As shown by Western analysis of mammary tissue lysates, a significant amount of phosphorylated Ron protein is present in mammary extracts from all the wild type and MT-Ron transgenic lines (Figure 5B, and data not shown). This increased Ron phosphorylation is similar to the overexpression and increased receptor phosphorylation observed in human breast cancers and suggests that Ron activation may be driving cell proliferation and survival signals.

To examine the downstream signaling pathways regulated in response to Ron activation, we analyzed the protein expression patterns of signaling molecules involved in cell cycle progression and survival. Normal mammary tissue from Tg- mice was compared to mammary tumor tissue taken from various Tg+ lines by Western analysis. Figure 5C illustrates the consistent increases observed in key signaling molecules, namely increases in β-catenin, cyclin D1, and c-Myc, found in the Ron-mediated breast tumors. In addition, increased amounts of phosporylated MAPK were observed.

The morphology of the Ron induced mammary tumors have striking similarities to tumors that develop in β-catenin overexpressing animal models (31, 32). These data suggest that Ron and β-catenin signaling may cooperate to produce very aggressive mammary tumors. To elucidate the

interaction of Ron and β-catenin, we performed immunoprecipitations of lysates from Tg- and Tg+ mammary tissue using antibodies directed against β-catenin, Ron, and IgG. Western membranes of the immune complexes were blotted with antibodies for Ron and phospho-Ron to assess the association of active (phosphorylated) Ron with β-catenin. As shown in Figure 6A, β-catenin associates with Ron and phospho-Ron as evident by the high protein expression in the Tg+ mammary tissue. To determine if this association is present for Ron as well, we conversely immunoprecipitated with Ron and blotted for Ron, β-catenin, and phospho-tyrosine. Western analyses indicate that β-catenin and Ron co-precipitate from transgenic mammary cell lysates and that β-catenin appears to be tyrosine phosphorylated in this complex (Figure 6B). Moreover, a high level of tyrosine phosphorylation was observed in the mammary tissue lysates. To determine if the increased amount of β-catenin observed in the mammary cell lysate was associated with an increase in the activation of β-catenin target genes, electromobility shift assays were performed utilizing a consensus β-catenin/TCF/LEF binding sequence. For these analyses, mammary tumor (Tg+) and non-transgenic mammary tissue (Tg-) lysates were incubated with a probe specific for the β-catenin/TCF binding site (Figure 6C). A protein:DNA complex is present when mammary tumor extract alone or in combination with non-specific inhibitor are incubated in the reaction. To test for binding specificity, a 100-fold excess of unlabeled specific or nonspecific competitor was added to the reaction. As is apparent in Figure 6C, the specific competitor efficiently competes the binding complex while the nonspecific competitor has no effect. To determine if β-catenin was present in the protein:DNA complex from the transgenic mammary tumor lysates, the addition of anti-β-catenin antibody was added to the reaction. With this addition, we saw a band shift as a result of the β-catenin/anti-β-catenin complex migrating toward the top of the gel (Figure 6C and data not shown). Relatively no active β-catenin complexes were seen in the Tg- mammary gland lysates, further supporting the upregulation and transcriptional activation of β-catenin in the mammary extracts from the Ron overexpressing glands (Figure 6 C).

Discussion

Overexpression of Ron is associated with human breast cancer and is found in a significant percentage of infiltrating carcinomas (8). In this study, we examined the effect of overexpressing the Ron receptor in the mammary epithelium. Our studies provide the first *in vivo* evidence that Ron overexpression in the mammary gland is sufficient to induce the onset of mammary tumors with a short latency and a highly metastatic phenotype. This data suggests that Ron participates in mammary cell transformation, cell dissociation and migration leading to a high degree of metastasis to distant secondary tissues. Tumorigenesis in these transgenic mouse lines was correlated with elevated expression of Ron and an increase in Ron-associated tyrosine kinase activity within the mammary gland. Ron overexpression produced mammary tumors in 100% of the transgenic mice and distant metastatic foci in about 90% of the animals assessed. Moreover, mammary tumor lysates isolated from transgenic mice display increased β-catenin expression and upregulated β-catenin target genes *cyclin D1* and *c-myc*. Our experimental observations support the clinical observations that Ron overexpression is associated with poor clinical outcome (8, 9) and a more aggressive phenotype as shown in a variety of *in vitro* assays (13, 19).

Constitutively active splice variants of Ron have also been identified in human colon cancer cell lines and tissues (33-35), making Ron an obvious target for further understanding aggressive disease. Therefore, we produced and characterized various transgenic lines that overexpress either the wild type form of Ron or the constitutively active form of Ron within the mammary gland to assess and better understand the biology behind Ron overexpression. The Ron transgene constructs were driven by the well characterized MMTV promoter, which produced high expression of Ron within the mammary gland and displayed no detectable expression in most other tissues. However, we detected minimal expression in the lacrimal gland which is consistent with the tissue-specific pattern of transgene expression in other MMTV-driven systems (36). The effect of Ron overexpression within

the mammary gland is evident by 12 weeks of age, inducing a mammary phenotype consisting of thick ductal branches, decreased side-branching, and the development of hyperplastic alveolar nodules. The hyperplastic nodules quickly form palpable mammary tumors in a majority of the transgenic mice by 8 months of age. These results are similar to what has been reported for the well-documented MMTV-*neu* animal model (37). However, the presence of metastatic foci in the lungs and liver of such a high percentage of transgenic mice is unique to this model of Ron overexpression.

As previously reported, Ron expression is barely detectable in normal mammary epithelial cells and benign breast lesions, but is overexpressed or constitutively activated in 50% of primary breast cancers (8). We have shown similar results in this transgenic model of breast cancer in which Ron expression was not detectable in non-transgenic mammary tissue and increased significantly in lysates from palpable mammary tumors. It has been suggested that Ron promotes invasive growth but does not initiate or participate in the early stages of transformation (9, 13). Our experimental data would suggest otherwise, showing the oncogenic potential of Ron when overexpressed, inducing mammary gland transformation and promoting invasive growth characteristics *in vivo*. We suggest that Ron participates in the early stages of mammary gland transformation as well as assists in the progression of mammary tumor growth and a highly metastatic phenotype.

The mammary tumors that developed as a result of Ron overexpression had an appearance that was variable, consisting of adenocarcinomas with varying degrees of desmoplastic epithelial malignancy. The tumors that developed as a result of Ron overexpression had a high degree of pleomorphism and an increase in the nuclear to cytoplasmic ratio which closely mimics what is observed in more aggressive human breast cancers. Furthermore, these tumors resembled the complex carcinomas that arise due to mutations in the Wnt signaling pathway, including mice with Wnt-1, Wnt-10b, β-catenin transgenes and APC mutations (31, 32). Characteristic of these Wnt-pathway induced tumors are well-developed stroma, myoepithelial and acinar glandular differentiation, and squamous metaplasia. The histological phenotype of our tumors suggest altered Wnt signaling, which is further

supported by our molecular studies showing an up-regulation of β-catenin and various target genes of the Wnt signaling pathway.

Regardless of the variable morphology, the tumors were uniformly aggressive and metastatic. The unexpected finding that a majority of the mice contained distant metastases may have important clinical implications. Many metastatic lesions were found in the vessels of the lungs and liver and some were also shown invading normal lung and liver tissue, suggesting that Ron overexpression increases cell motility/invasiveness *in vivo*, which has been previously suggested by *in vitro* invasion assays (35, 38, 39).

To support the cooperative involvement of Ron and β-catenin, we showed evidence that active Ron associates with β-catenin and elevates expression of β-catenin target genes. Previous reports have shown that oncogenic mutants of the MET family have the ability to activate the β-catenin pathway when expressed in NIH3T3 or Madin-Darby canine kidney cells (17). In support of our work which shows an up-regulation of β-catenin as a result of Ron overexpression, Buillions and Levine showed *in vitro* that activated Ron causes a tyrosine phosphorylation of β-catenin that correlates with an increase in cytoplasmic β-catenin and consequent transcriptional activation via TCF-4 transcription factor leading to the up-regulation of *c-myc* and *cyclin D1* gene expression (12). We also showed that β-catenin was present and capable of binding the TCF/LEF transcription site found upstream of various target genes that were upregulated due to Ron overexpression. Furthermore, silencing of Ron gene expression in colon cancer cell lines leads to diminished β-catenin expression (40). These studies and ours suggest that the β-catenin pathway may be involved in Ron-mediated tumorigenesis in the mammary gland.

Additionally, Ron overexpressing mammary tumors also showed an activated MAPK pathway that has been previously shown to be essential for cell transformation by MET (41-43), suggesting that Ron overexpression may induce or associate with various pathways required for mammary tumor initiation and progression. The association of Ron with various signaling cascades involving cell

proliferation and survival suggests that mammary cells overexpressing Ron may have a survival advantage in the environment associated with invasion and distant metastasis. Further understanding the interaction of Ron, β-catenin and other critical signaling modalities within mammary epithelial cells will offer a better understanding into how to treat Ron overexpressing tumors that have a highly metastatic phenotype.

Acknowledgements: The authors would like to acknowledge Jerilyn Girardi for her contribution to the mouse colony and Dr. James Lessard for the gift of the actin antibody. This work was supported in part by Public Health Service Grants CA100002 (S.E.W.) and DK073552 (S.E.W.), the Digestive Diseases Research Development Center grant DK064403 (S.E.W. and M.A.L.), a NCI Core Phenotyping Award (R24 CA95784) from the National Institutes of Health, a Career Development Award #DAMD17-02-1-0342 from the Department of Defense (S.E.W.), and a Children's Digestive Health and Nutrition Foundation Young Investigator Development Award (M.A.L). The authors have no conflicting financial interests.

References

1. Shien T, Tashiro T, Omatsu M, et al. Frequent overexpression of epidermal growth factor receptor (EGFR) in mammary high grade ductal carcinomas with myoepithelial differentiation. J Clin Pathol 2005;58(12):1299-304.

2. Carvalho I, Milanezi F, Martins A, Reis RM, Schmitt F. Overexpression of platelet-derived growth factor receptor alpha in breast cancer is associated with tumour progression. Breast Cancer Res 2005;7(5):R788-95.

3. Born M, Quintanilla-Fend L, Braselmann H, et al. Simultaneous over-expression of the Her2/neu and PTK6 tyrosine kinases in archival invasive ductal breast carcinomas. J Pathol 2005;205(5):592-6.

4. Hennipman A, van Oirschot BA, Smits J, Rijksen G, Staal GE. Tyrosine kinase activity in breast cancer, benign breast disease, and normal breast tissue. Cancer Res 1989;49(3):516-21.

5. La Rosa S, Sessa F, Colombo L, Tibiletti MG, Furlan D, Capella C. Expression of acidic fibroblast growth factor (aFGF) and fibroblast growth factor receptor 4 (FGFR4) in breast fibroadenomas. J Clin Pathol 2001;54(1):37-41.

6. Meng S, Tripathy D, Shete S, et al. HER-2 gene amplification can be acquired as breast cancer progresses. Proc Natl Acad Sci U S A 2004;101(25):9393-8.

7. Shimizu C, Hasegawa T, Tani Y, et al. Expression of insulin-like growth factor 1 receptor in primary breast cancer: immunohistochemical analysis. Hum Pathol 2004;35(12):1537-42.

8. Maggiora P, Marchio S, Stella MC, et al. Overexpression of the RON gene in human breast carcinoma. Oncogene 1998;16(22):2927-33.

9. Lee WY, Chen HH, Chow NH, Su WC, Lin PW, Guo HR. Prognostic significance of co-expression of RON and MET receptors in node-negative breast cancer patients. Clin Cancer Res 2005;11(6):2222-8.

10. Iwama A, Yamaguchi N, Suda T. STK/RON receptor tyrosine kinase mediates both apoptotic and growth signals via the multifunctional docking site conserved among the HGF receptor family. Embo J 1996;15(21):5866-75.

11. Xiao ZQ, Chen YQ, Wang MH. Requirement of both tyrosine residues 1330 and 1337 in the C-terminal tail of the RON receptor tyrosine kinase for epithelial cell scattering and migration. Biochem Biophys Res Commun 2000;267(2):669-75.

12. Bullions LC, Levine AJ. The role of beta-catenin in cell adhesion, signal transduction, and cancer. Curr Opin Oncol 1998;10(1):81-7.

13. Santoro MM, Collesi C, Grisendi S, Gaudino G, Comoglio PM. Constitutive activation of the RON gene promotes invasive growth but not transformation. Mol Cell Biol 1996;16(12):7072-83.

14. Wang MH, Montero-Julian FA, Dauny I, Leonard EJ. Requirement of phosphatidylinositol-3 kinase for epithelial cell migration activated by human macrophage stimulating protein. Oncogene 1996;13(10):2167-75.

15. Mera A, Suga M, Ando M, Suda T, Yamaguchi N. Induction of cell shape changes through activation of the interleukin-3 common beta chain receptor by the RON receptor-type tyrosine kinase. J Biol Chem 1999;274(22):15766-74.

16. Waltz SE, McDowell SA, Muraoka RS, et al. Functional characterization of domains contained in hepatocyte growth factor-like protein. J Biol Chem 1997;272(48):30526-37.

17. Danilkovitch-Miagkova A, Miagkov A, Skeel A, Nakaigawa N, Zbar B, Leonard EJ. Oncogenic mutants of RON and MET receptor tyrosine kinases cause activation of the beta-catenin pathway. Mol Cell Biol 2001;21(17):5857-68.

18. Schmidt L, Junker K, Weirich G, et al. Two North American families with hereditary papillary renal carcinoma and identical novel mutations in the MET proto-oncogene. Cancer Res 1998;58(8):1719-22.

19. Peace BE, Hughes MJ, Degen SJ, Waltz SE. Point mutations and overexpression of Ron induce transformation, tumor formation, and metastasis. Oncogene 2001;20(43):6142-51.

20. Santoro MM, Penengo L, Minetto M, Orecchia S, Cilli M, Gaudino G. Point mutations in the tyrosine kinase domain release the oncogenic and metastatic potential of the Ron receptor. Oncogene 1998;17(6):741-9.

21. Iwama A, Okano K, Sudo T, Matsuda Y, Suda T. Molecular cloning of a novel receptor tyrosine kinase gene, STK, derived from enriched hematopoietic stem cells. Blood 1994;83(11):3160-9.

22. Waltz SE, Toms CL, McDowell SA, et al. Characterization of the mouse Ron/Stk receptor tyrosine kinase gene. Oncogene 1998;16(1):27-42.

23. Omer CA, Chen Z, Diehl RE, et al. Mouse mammary tumor virus-Ki-rasB transgenic mice develop mammary carcinomas that can be growth-inhibited by a farnesyl:protein transferase inhibitor. Cancer Res 2000;60(10):2680-8.

24. Hofstra RM, Landsvater RM, Ceccherini I, et al. A mutation in the RET proto-oncogene associated with multiple endocrine neoplasia type 2B and sporadic medullary thyroid carcinoma. Nature 1994;367(6461):375-6.

25. Jeffers M, Schmidt L, Nakaigawa N, et al. Activating mutations for the met tyrosine kinase receptor in human cancer. Proc Natl Acad Sci U S A 1997;94(21):11445-50.

26. Longati P, Bardelli A, Ponzetto C, Naldini L, Comoglio PM. Tyrosines1234-1235 are critical for activation of the tyrosine kinase encoded by the MET proto-oncogene (HGF receptor). Oncogene 1994;9(1):49-57.

27. Longley BJ, Tyrrell L, Lu SZ, et al. Somatic c-KIT activating mutation in urticaria pigmentosa and aggressive mastocytosis: establishment of clonality in a human mast cell neoplasm. Nat Genet 1996;12(3):312-4.

28. Schmidt L, Duh FM, Chen F, et al. Germline and somatic mutations in the tyrosine kinase domain of the MET proto-oncogene in papillary renal carcinomas. Nat Genet 1997;16(1):68-73.

29. Niemann C, Brinkmann V, Spitzer E, et al. Reconstitution of mammary gland development in vitro: requirement of c-met and c-erbB2 signaling for branching and alveolar morphogenesis. J Cell Biol 1998;143(2):533-45.

30. Yant J, Buluwela L, Niranjan B, Gusterson B, Kamalati T. In vivo effects of hepatocyte growth factor/scatter factor on mouse mammary gland development. Exp Cell Res 1998;241(2):476-81.

31. Miyoshi K, Rosner A, Nozawa M, et al. Activation of different Wnt/beta-catenin signaling components in mammary epithelium induces transdifferentiation and the formation of pilar tumors. Oncogene 2002;21(36):5548-56.

32. Rosner A, Miyoshi K, Landesman-Bollag E, et al. Pathway pathology: histological differences between ErbB/Ras and Wnt pathway transgenic mammary tumors. Am J Pathol 2002;161(3):1087-97.

33. Collesi C, Santoro MM, Gaudino G, Comoglio PM. A splicing variant of the RON transcript induces constitutive tyrosine kinase activity and an invasive phenotype. Mol Cell Biol 1996;16(10):5518-26.

34. Okino T, Egami H, Ohmachi H, et al. Presence of RON receptor tyrosine kinase and its splicing variant in malignant and non-malignant human colonic mucosa. Int J Oncol 1999;15(4):709-14.

35. Wang MH, Kurtz AL, Chen Y. Identification of a novel splicing product of the RON receptor tyrosine kinase in human colorectal carcinoma cells. Carcinogenesis 2000;21(8):1507-12.

36. Webster MA, Hutchinson JN, Rauh MJ, et al. Requirement for both Shc and phosphatidylinositol 3' kinase signaling pathways in polyomavirus middle T-mediated mammary tumorigenesis. Mol Cell Biol 1998;18(4):2344-59.

37. Guy CT, Webster MA, Schaller M, Parsons TJ, Cardiff RD, Muller WJ. Expression of the neu protooncogene in the mammary epithelium of transgenic mice induces metastatic disease. Proc Natl Acad Sci U S A 1992;89(22):10578-82.

38. Chen YQ, Zhou YQ, Angeloni D, Kurtz AL, Qiang XZ, Wang MH. Overexpression and activation of the RON receptor tyrosine kinase in a panel of human colorectal carcinoma cell lines. Exp Cell Res 2000;261(1):229-38.

39. Zhou YQ, He C, Chen YQ, Wang D, Wang MH. Altered expression of the RON receptor tyrosine kinase in primary human colorectal adenocarcinomas: generation of different splicing RON variants and their oncogenic potential. Oncogene 2003;22(2):186-97.

40. Xu XM, Wang D, Shen Q, Chen YQ, Wang MH. RNA-mediated gene silencing of the RON receptor tyrosine kinase alters oncogenic phenotypes of human colorectal carcinoma cells. Oncogene 2004;23(52):8464-74.

41. Bardelli A, Longati P, Gramaglia D, et al. Uncoupling signal transducers from oncogenic MET mutants abrogates cell transformation and inhibits invasive growth. Proc Natl Acad Sci U S A 1998;95(24):14379-83.

42. Jeffers M, Fiscella M, Webb CP, Anver M, Koochekpour S, Vande Woude GF. The mutationally activated Met receptor mediates motility and metastasis. Proc Natl Acad Sci U S A 1998;95(24):14417-22.

43. Rodrigues GA, Park M, Schlessinger J. Activation of the JNK pathway is essential for transformation by the Met oncogene. Embo J 1997;16(10):2634-45.

Figure Legends

Figure 1. Characterization of the MMTV-Ron Transgenic Mice. A. Generation and targeted expression of Ron in the mammary gland of transgenic mice. Expression cassette used for the generation of the wild type Ron (WT-Ron) and constitutively active Ron (ΔM1231T, MT-Ron) mice. Wild type murine Ron (mRon) transgene (bottom) driven by the mouse mammary tumor virus (MMTV) promoter (grey box) was constructed as described in the Experimental procedures. This MMTV mRon transgene harbors the first three exons (black boxes) and introns (horizontal black line) of wild type mRon genomic DNA followed by, in the correct reading frame, exons 4-19 of wild type mRon cDNA. The location of a 706 bp genomic DNA probe used in Southern analyses to differentiate transgenic from endogenous wild type mRon of transgenic mice is noted below the mRon gene figure (top). The open arrow indicates the location of the ΔM1231T point mutation generated from the mRon cDNA sequence which leads to a constitutively active mRon tyrosine kinase. Restriction enzyme cut sites: A, Age I; B, BamHI; E, EcoRI; N, Not I; P, PmeI; S, Spe I; X, Xho I. A 2.0 kb ruler is noted at right. **B**. Ron transgene expression in the mammary gland of transgenic mice. Whole cell lysates from various tissues taken from transgenic (Tg+) and non-transgenic (Tg-) mice were used to assess the level of Ron protein expression. Lysates were subjected to SDS-PAGE and blotted with a polyclonal antibody that recognizes the Ron β chain. Ron is highly expressed in the mammary gland of transgenic mice and is also detectable in the lacrimal gland of MMTV-Ron mice (right panel). Detection of Ron was not evident in non-transgenic tissues (left panel). The membranes were stripped and re-probed with anti-actin antibody to ensure equal protein loading. MG- mammary gland, Kid-Kidney, Lg- Lung, Spl- Spleen, Sk- skin, Li-Liver, LG- lacrimal gland, SG- Salivary gland. **C.** Histological differences in lacrimal glands. Enlarged lacrimal glands in MMTV-Ron transgenic animals (**b** and **d**) showed extremely dilated, cystic acini lined by hyperplastic epithelial cells (**d**). This

dysplastic architecture is vastly different from that observed in wild type animals (**a** and **c**). Bar represents 200μM.

Figure 2. Mammary-specific expression of the MMTV-Ron transgene induces mammary hyperplasia and alveolar development. **A** and **B:** Whole mounts from 12-week old nulliparous non-transgenic (**A**) and MMTV-Ron (WT-Ron) (**B**) mice. The mammary-specific expression of MMTV-Ron produced acinar hyperplasia and distended ductal morphology (**B**) compared to non-transgenic tissue which shows normal glandular morphology with thin ducts and abundant secondary and tertiary branches (**A**). **C** and **D:** Hematoxylin and eosin stained sections of mammary gland from wild type mice showing normal glandular morphology with thin ducts (arrowhead) (**C**) and from transgenic glands showing epithelial hyperplasia (block arrow) and secretory vacuolization with distended ducts (arrow) (**D**). Bar represents 200μm (A and B) or 100μm (C and D).

Figure 3. Expression of WT-Ron and MT-Ron in mammary gland induces tumor formation. **A:** Kinetics of mammary tumor development in WT-Ron and MT-Ron mice. Transgenic lines had a similar tumor incidence but had a tumor latency that was significantly shorter in MT-Ron mice with median tumor formation being 189 days compared to WT-Ron mice that had median tumor development time of 202 days. $p<0.05$. **B:** Expression of WT-Ron and MT-Ron in mammary gland induces a variety of mammary tumor phenotypes in transgenic mice. Representative mammary tumors from transgenic mice display phenotypes consistent with **a**) adenocarcinomas, characterized by large cells and regions of **b**) desmoplasia. **c**) Other tumor phenotypes resembled papillary myoepithelial carcinomas that display signs of **d**) localized invasion as tumor cells migrate through the underlying muscle tissue (arrow).

Figure 4. Presence of metastatic foci at distant sites in MMTV-Ron transgenic mice. A Representative illustrations of metastatic foci within the MMTV-Ron tissues. **a**: A gross representation of metastatic foci found in lung tissue derived from primary mammary tumors induced by Ron overexpression. **b:** Section of the lung displaying metastatic foci from the primary mammary tumor that developed as a result of Ron overexpression in the mammary gland. The metastatic foci were found growing in the vessels of the lung (*) as well as foci that have traversed the vessel wall to form a colony within the lung parenchyma (data not shown). **c:** Representative section of the liver also revealed metastatic foci. The foci found in the liver displayed similar growth characteristics to those found in the lung with metastatic cells associated with vessels and metastatic loci that were more invasive, migrating into the liver parenchyma with associated liver damage (hemorrhagic necrosis due to tumor associated vessel blockage). **d:** Immunohistochemistry was used to determine Ron expression status within the metastatic lung foci. Lung tissue was stained with an anti-Ron antibody which shows positive staining (Red) in the foci. **B.** Summary of metastatic foci as described in the Experimental Procedures Section.

Figure 5. Expression analysis of the mammary epithelium of MMTV-Ron transgenic mice. A: Northern hybridization analysis of RNA isolated from non-transgenic and transgenic mammary tissue analyzed for Ron expression. The level of Ron expression increases in palpable mammary tumor tissue (T) compared to mammary gland tissue without palpable mammary tumors (M) from transgenic animals. No expression is detected in non-transgenic mammary tissue (Tg-). Membranes were stripped and re-probed for GAPDH to ensure equal loading. **B:** Western analysis of protein isolated from tumor tissue of transgenic and mammary tissue of non-transgenic mice. Tissue extracts were assayed for total Ron expression. Membranes were then probed with a phospho-(p)Ron antibody to assess the amount of activated Ron expression in the tumor tissue compared to the normal mammary

gland. Membranes were stripped and re-probed with an antibody to actin C4 to control for protein loading. **C:** Ron overexpression elevates the level of β-catenin in tumor tissue and corresponding β-catenin target genes including *cyclin D1* and *c-myc*. Increased expression of activated [phospho-(p)]MAPK was observed compared to total MAPK expression which shows no change in the total MAPK expression between transgenic tumor tissue and non-transgenic mammary tissue. A significant increase of these cycling associated genes is only detected in transgenic tissue compared to non-transgenic tissue.

Figure 6. Immunoprecipitation of mammary tissue lysates showing an association between Ron and β-catenin. **A:** Whole cell lysates from non-transgenic (Tg-) and transgenic (Tg+) mammary tissue were immunoprecipitated with either an anti- β-catenin or mouse IgG. The precipitated immunocomplexes were then analyzed by Western analyses with anti-Ron and pRon antibodies. Activated Ron protein immunoprecipitates with β-catenin. **B:** The Ron and IgG precipitated immunocomplexes were further analyzed by Western analyses with anti-Ron, β-catenin, and p-tyrosine antibodies. A whole cell lysate control was provided to show total levels of each protein. **C:** Electromobility Shift Assays were performed using a consensus b̃catenin/TCF/LEF binding sequence. Mammary tissues extracts were loaded in the presence (+) or absence (-) of specific competitor, an antibody to β-catenin, or a non-specific competitor (non-specific probe). A strong protein:DNA complex was observed in mammary tumor tissue from the transgenic mice. This complex was specific for our target sequence and contained b-catenin. Minimal complex formation was observed in the non-transgenic mammary tissue.

Figure 1

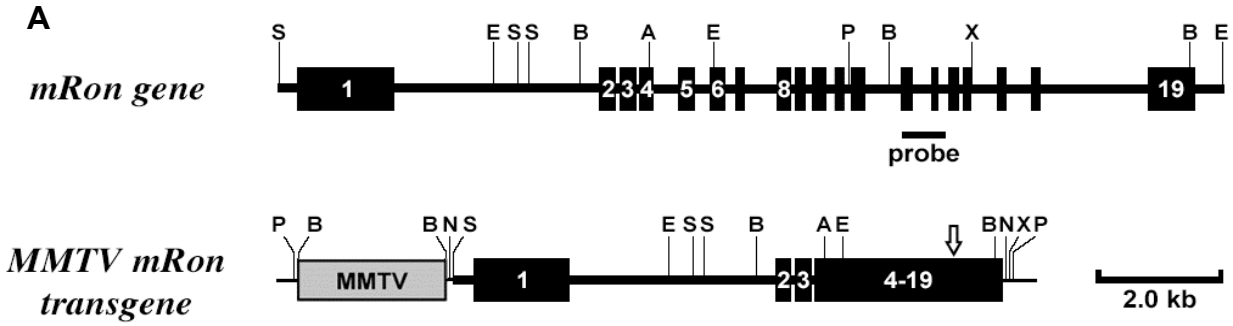
A
mRon gene
S
E S S
B
A
E
P
B
X
B E
1
2 3 4
5
6
8
19
probe
MMTV mRon transgene
P B
B N S
E S S
B
A E
B N X P
MMTV
1
2 3
4-19
2.0 kb

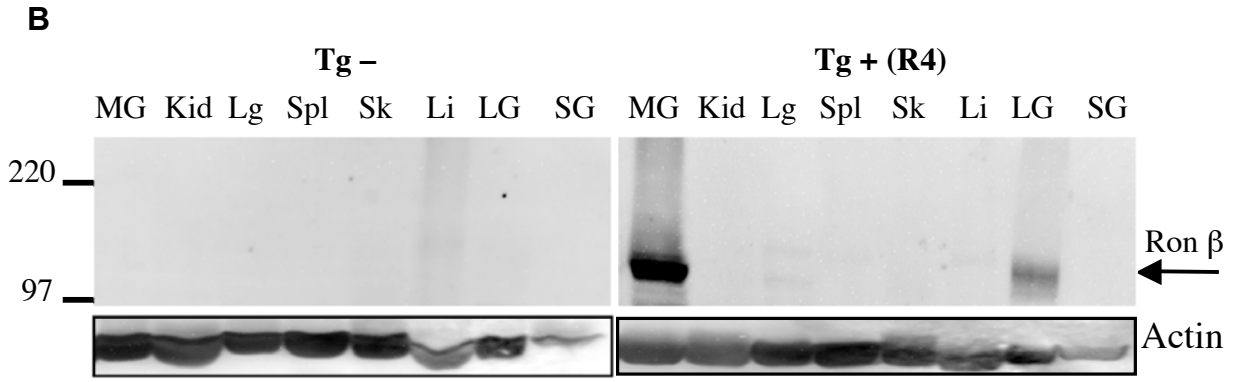
B
Tg –
Tg + (R4)
MG Kid Lg Spl Sk Li LG SG
MG Kid Lg Spl Sk Li LG SG
220
97
Ron β
Actin

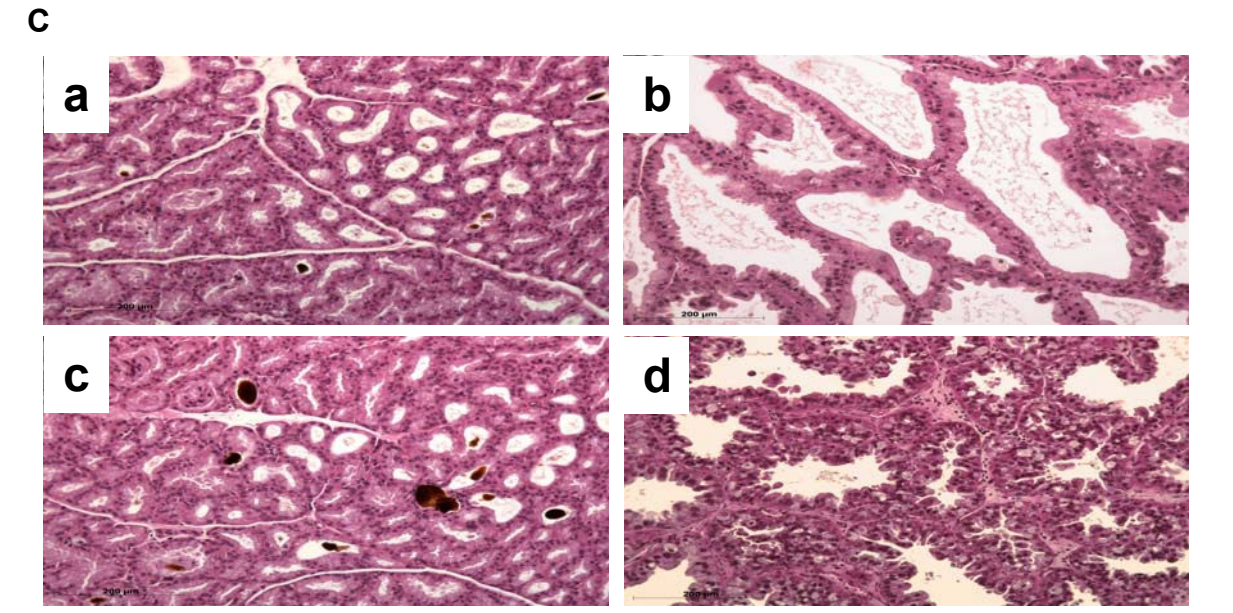
C
a
b
c
d

Figure 2

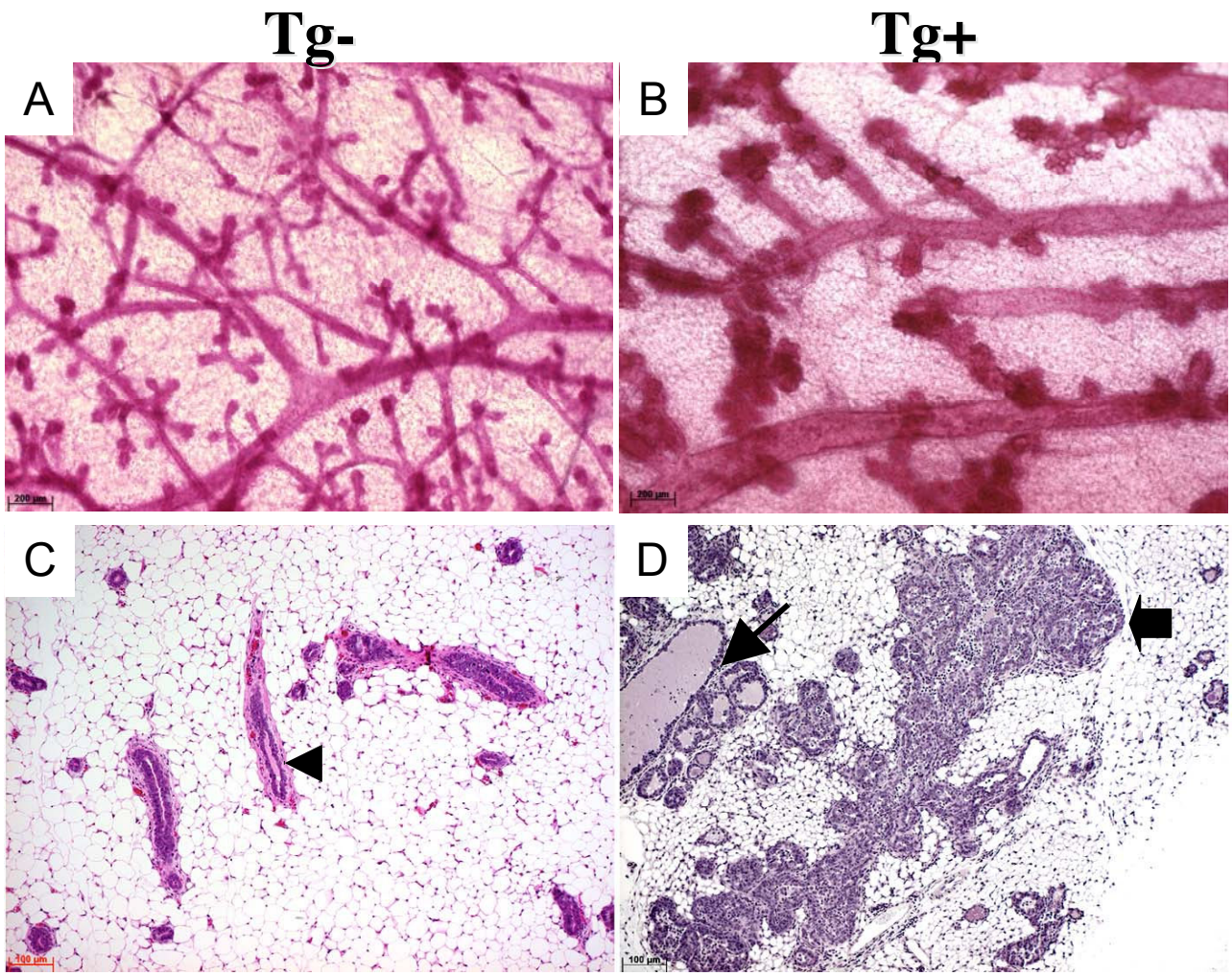

Figure 3

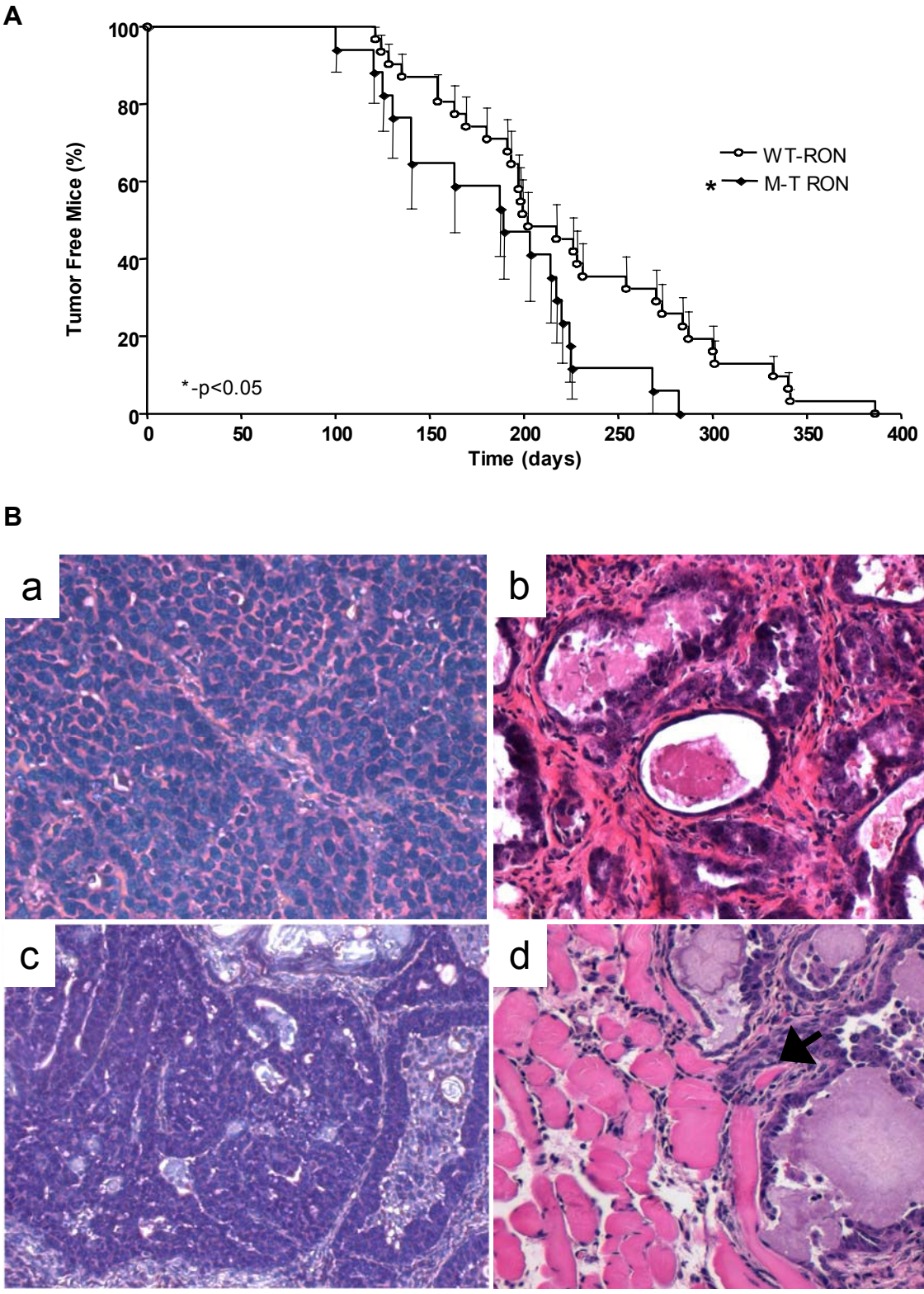
A
100
80
60
40
20
0
Tumor Free Mice (%)
0
50
100
150
200
250
300
350
400
Time (days)
WT-RON
M-T RON
*
*-p<0.05
B
a
b
c
d

Figure 4

A

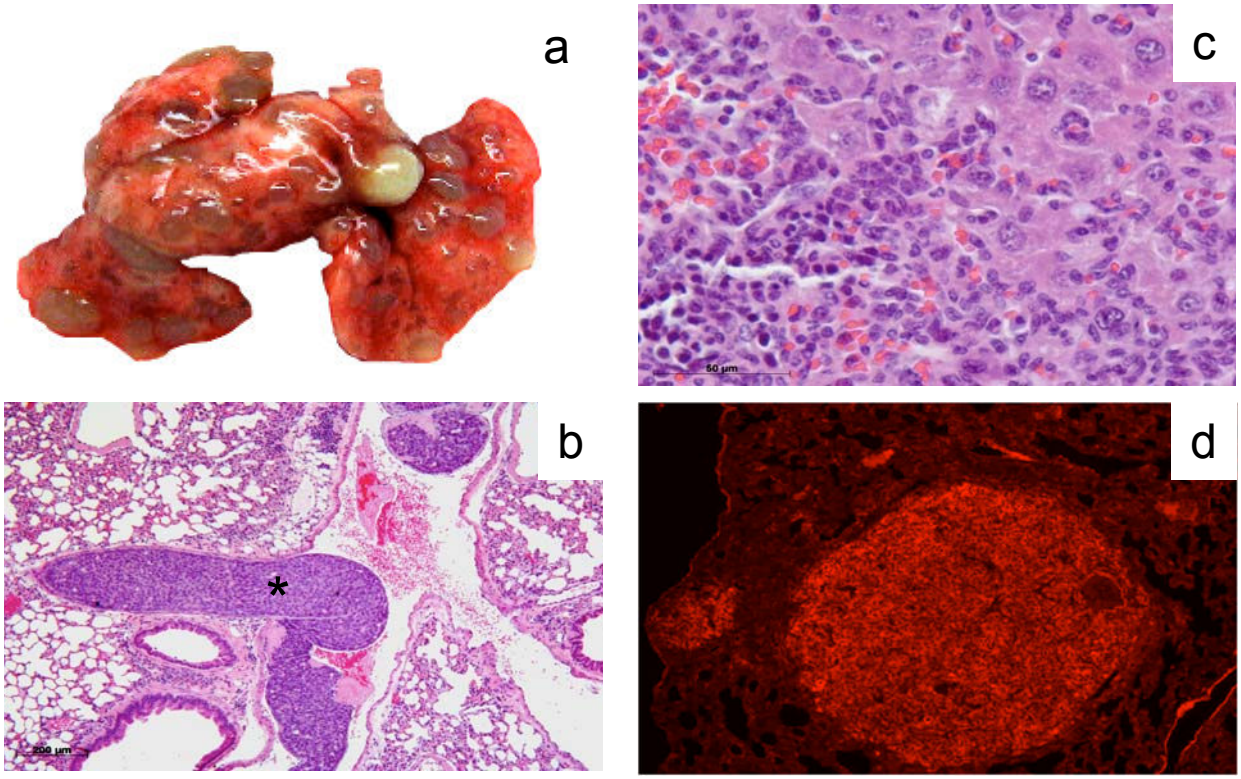

B

Mouse Line	% Mice with Lung Metastasis	% Mice with Liver Metastasis
WT-RON	89.7 (26/29)	86.4 (19/22)
MT-RON	94.1 (16/17)	90.9 (10/11)

Figure 5

A

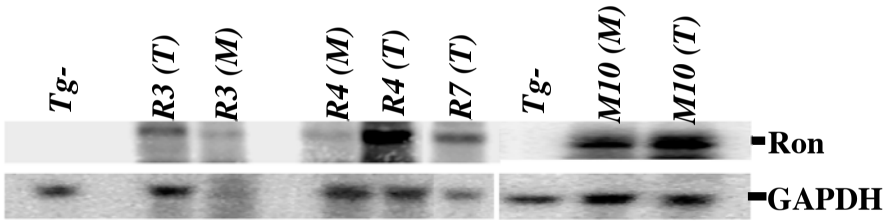
Tg-
R3 (T)
R3 (M)
R4 (M)
R4 (T)
R7 (T)
Tg-
M10 (M)
M10 (T)
Ron
GAPDH

B

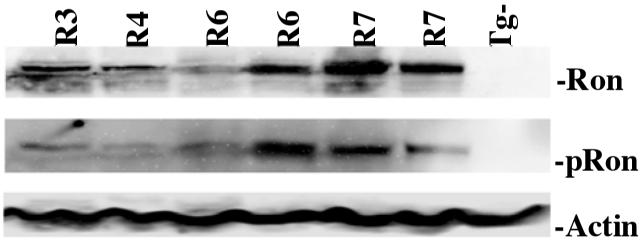
R3
R4
R6
R6
R7
R7
Tg-
-Ron
-pRon
-Actin

C

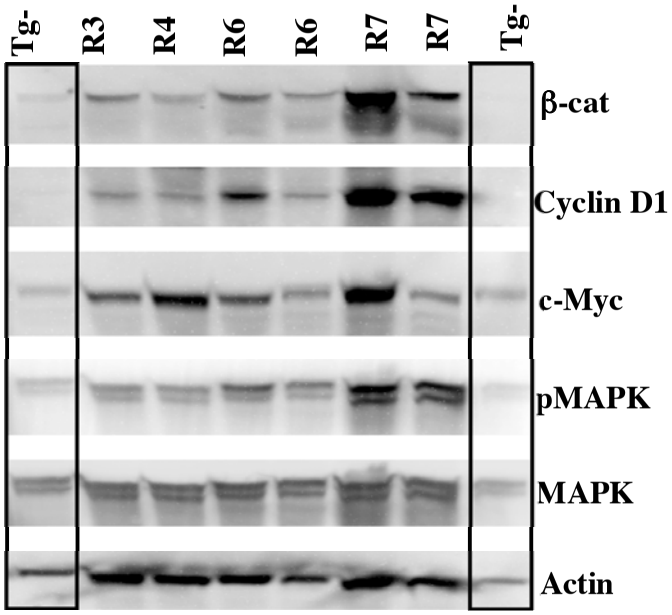
Tg-
R3
R4
R6
R6
R7
R7
Tg-
β-cat
Cyclin D1
c-Myc
pMAPK
MAPK
Actin

Figure 6

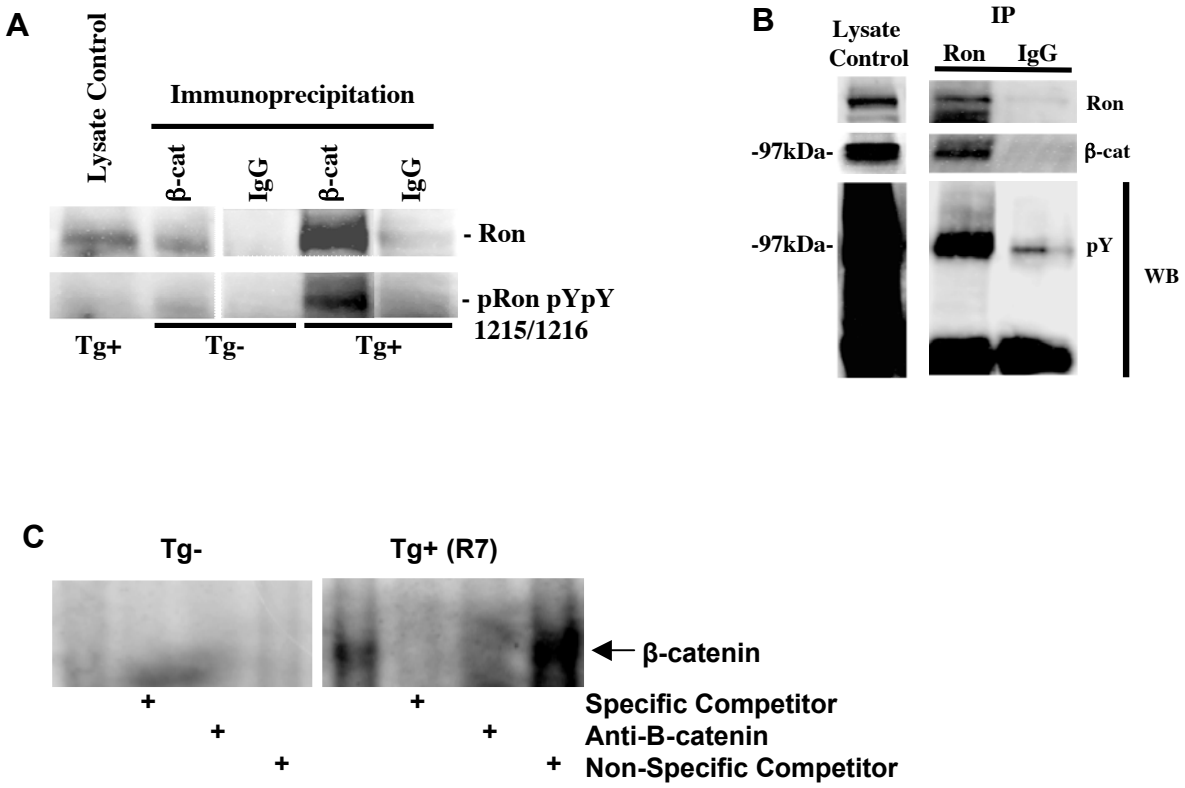
A
Lysate Control
Immunoprecipitation
β-cat
IgG
β-cat
IgG
- Ron
- pRon pYpY 1215/1216
Tg+
Tg-
Tg+
B
Lysate Control
IP
Ron
IgG
Ron
-97kDa-
β-cat
-97kDa-
pY
WB
C
Tg-
Tg+ (R7)
β-catenin
+
+
+
+
+
+
Specific Competitor
Anti-B-catenin
Non-Specific Competitor